in transplanted kidneys, despite all the recipients having renal failure secondary to diabetic nephropathy [6]. However, specific 'markers' within the kidney for predicting future decline in renal function remain to be established.

Connexins are integral membrane proteins that form hexamers called connexons. Two connexons located in the plasma membrane of adjacent cells form gap junctions, which are intercellular channels that permit the passage of small molecules such as small metabolites, ions and second messengers [7]. At least 20 rodent and 21 human connexins have been identified [7]. Among them, connexin43 (Cx43) is expressed most abundantly and by a variety of cell types [7]. In the kidney, nine connexins are known to be expressed: Cx26, Cx30.3, Cx31, Cx32, Cx37, Cx40, Cx43, Cx45 and Cx46 [8]. Previous studies have shown that Cx43 is expressed at podocytes in normal and diseased human kidney [9,10], but Cx43 expression in diabetic nephropathy and its significance remain totally unknown.

In this study, we examined the changes in glomerular Cx43 staining of type 2 diabetic patients with overt nephropathy, comparing them with normal controls. Furthermore, we investigated whether the magnitude of alteration in Cx43 expression at podocytes could be a prognostic marker for the progression of diabetic nephropathy.

Subjects and methods

Subjects

Needle renal biopsy tissues of 29 type 2 diabetic patients with overt nephropathy were obtained from those treated between 1999 and 2005 at Kyoto University Hospital or at Saiseikai Nakatsu Hospital. The patients underwent renal biopsy because of the presence of haematuria, and/or the absence of retinopathy, and/or a known history of diabetes. The presence of overt diabetic nephropathy was confirmed based on established criteria [5]. No patient received steroids or immunosuppressive drugs. The patients were followed up for 10–49 months (mean, 23±3 months). For normal controls, tissues obtained from seven subjects using uninvolved portions of surgically removed kidneys afflicted with localized neoplasm, and five biopsy samples from patients with minor glomerular abnormalities were used. Histopathological examination of control tissues excluded any glomerular diseases. The samples were fixed in Dubosq–Brazil solution and embedded in paraffin. Table 1 summarizes the details of the analysed materials. This study was approved by the Human Research Committee of Kyoto University Graduate School of Medicine.

Immunohistochemistry

Immunohistochemical analysis for Cx43 and Wilms' tumor-1 (WT1) was performed as previously described [4] with some modifications. In brief, deparaffinized 3 μm kidney sections were treated with autoclave heating (10 min in 10 mM citrate buffer, pH 6.0). After blocking of endogenous peroxidase with 1.5% H_2O_2 for 15 min at 22°C, sections were incubated with 1% Triton-X in phosphate-buffered saline (PBS) for 20 min at 22°C, washed three times with PBS for 5 min and incubated with 10% normal goat or donkey serum in PBS for 10 min. Rabbit antibodies against Cx43 (C-6219, Sigma-Aldrich, St. Louis, USA) or human WT1 (sc-192, Santa Cruz Biotechnology, Santa Cruz, USA) were diluted 1:50 in PBS containing 1% bovine serum albumin (1% BSA/PBS), and the mixture was incubated for 1 h at 22°C. For Cx43 staining, after incubation with streptavidin-horseradish peroxidase (HRP) (DakoCytomation, Kyoto, Japan) for 20 min at 22°C, the sections were incubated with anti-rabbit biotin (Vector, Burlingame, USA) for 30 min at 22°C. The sections were processed with 3,3′-diaminobenzidine and counterstained with hematoxylin. For WT1 staining, after blocking of endogenous phosphatase by incubation with 2 mM levamisole for 5 min three times at 22°C, the sections were incubated with alkaline phosphatase-conjugated secondary antibodies (711-055-152, donkey anti-rabbit IgG, Jackson ImmunoResearch, West Grove, USA) diluted 1:100 in 1% BSA/PBS for 30 min at 22°C. The sections were processed with nitroblue tetrazolium-bromochloroindolylphosphate toluidine (1-697-471, Roche Diagnostics, Mannheim, Germany) in alkaline buffer (100 mM Tris, pH 9.5, 100 mM NaCl, 50 mM $MgCl_2$) and counterstained with Kernechtrot Stain Solution (Muto Pure Chemicals, Tokyo, Japan). Non-immune rabbit serum was used as negative controls.

Evaluation of Cx43 staining

Evaluation of Cx43 staining was classified by the intensity of Cx43 staining as scores 0–4 (0, no expression detectable;

Table 1. Clinical features of patients at renal biopsy

Diagnosis	*n*	Gender (M/F)	Age (years)	sCr (mg/dl)	BUN (mg/dl)	Urinary protein (g/gCr)	Ccr (ml/min)	HbA1c (%)	SBP (mmHg)	DBP (mmHg)	mBP (mmHg)
Controls	12	2/10	55±6	0.70±0.04	14.8±1.2	0.06±0.02	100±11	5.0±0.3	115±4	70±3	85±3
Nephrectomy	7	2/5	68±5	0.79±0.04	16.9±1.3	0.04±0.01	95±23	5.2±0.4	123±5	76±2	92±3
Minor glomerular abnormalities	5	0/5	36±8	0.58±0.04	11.8±1.6	0.08±0.03	103±9	4.8±0.1	104±3	60±2	75±1
Diabetic nephropathy	29	22/7	59±2	1.35±0.12	24.2±2.0	6.14±0.96	55±9	6.8±0.5	140±5	76±3	97±3
P-value DN *vs* controls			NS	$P<0.005$	$P<0.05$	$P<0.0001$	$P<0.005$	$P<0.005$	$P<0.005$	NS	$P<0.05$

Data are means±SEM unless otherwise indicated. sCr, serum creatinine; BUN, blood urea nitrogen; Ccr, creatinine clearance; SBP, systolic blood pressure; DBP, diastolic blood pressure; mBP, mean blood pressure; DN, diabetic nephropathy; NS, non-significant.

1, only weak expression; 2, detectable expression; 3, high expression as observed in normal controls; 4, highest expression, higher than normal controls) and by the degree of Cx43 heterogeneity, defined as the loss of uniformly linear Cx43 staining pattern due to segmental thickening, thinning and loss of Cx43 staining, as scores 0–3 (0, without heterogeneity as in normal controls; 1, segmental heterogeneity, segmental heterogeneity with conservation of more than half of glomerular linear Cx43 staining; 2, moderate heterogeneity, heterogeneity with less than half of glomerular linear Cx43 staining; 3, global heterogeneity, global heterogeneity with almost no preservation of linear Cx43 staining; see Figures 1 and 2 for representative Cx43 staining). Examination of Cx43 staining intensity and Cx43 heterogeneity was done by two independent reviewers using normal controls and representative diabetic nephropathy samples as relative standards, and the scores were averaged. At least six glomeruli per biopsy were evaluated at high-power magnification, and the scores were averaged.

The number of podocytes per glomerulus cross section was determined by the mean number of WT1-positive cell number per glomerular cross section, excluding parietal epithelial cells.

Cell culture and western blotting

A conditionally immortalized human podocyte was cultured as described previously [11]. In brief, these cells proliferate when cultured at 33°C, whereas they halt growing and begin to differentiate to express podocyte-specific genes when cultured at 37°C. Podocytes were cultured with RPMI 1640 medium (Sigma-Aldrich) supplemented with 10% fetal calf serum (FCS, Sigma-Aldrich) and insulin–transferrin–sodium selenite media supplement (Sigma-Aldrich). Cells were differentiated at 37°C for 2 weeks without passage, and cultured with RPMI 1640 containing 10% FCS with 5.5 mM glucose (normal glucose) or 25 mM glucose (high glucose) for 8 days. Cells were used between passages 15 and 18.

Western blot analysis was performed as described [4]. After incubation with 50% trichloroacetic acid on ice for 10 min, cells were centrifuged at 15 000 × *g*. Precipitations were resuspended in sample buffer containing 2% 2-mercaptoethanol, 125 mM Tris, 20% glycerol, 0.001% bromophenol blue and 4% sodium dodecyl sulfate (SDS), and separated by 10% SDS-polyacrylamide gel electrophoresis and transferred onto nitrocellulose membrane (Bio-Rad, Hercules, USA). After incubation with rabbit antibodies against Cx43 (C-6219, Sigma-Aldrich) or mouse antibodies against β-actin (A-2547, Sigma-Aldrich), immunoblots were developed with HRP-conjugated anti-rabbit IgG (Amersham, Arlington Heights, USA) or HRP-conjugated anti-mouse antibody (Santa Cruz) and LumiGLO Reagent (Cell Signaling Technology, Danvers, USA).

Statistics

Data are expressed as means ± SEM, unless otherwise indicated. Correlation coefficients were calculated by Spearman's method, and between-group differences were determined by ANOVA with Kruskal–Wallis method.

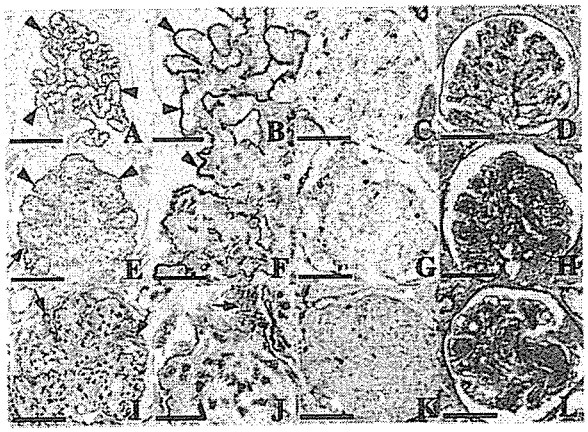

Fig. 1. Cx43 staining in normal control and in diabetic nephropathy. Cx43 staining (**A**, **B**, **E**, **F**, **I**, **J**, stained with anti-Cx43 antibody, brown), WT1 staining (**C**, **G**, **K**, stained with anti-WT1 antibody, purple), and Periodic acid-Schiff (PAS) staining (**D**, **H**, **L**) in normal controls (**A–D**) and in diabetic patients (**E–L**) are shown. Podocytes are detected as nuclear WT1 positive cells outside the glomerular basement membrane (GBM) (**C**, **G**, **K**, white arrows). In normal controls, Cx43 staining in podocytes showed a linear to fine granular pattern along the GBM (**A**, **B**, black arrowheads). In case 1 (sCr 0.8 mg/dl at the time of biopsy and has a stable glomerular function after 3 years, **E–H**, Cx43 heterogeneity score, 1; Cx43 intensity score, 2), partial loss of Cx43 (**F**, white arrowhead) was present but the Cx43 staining pattern seems uniform. In contrast, in case 2 (sCr 0.8 mg/dl at the time of biopsy, but reached end-stage renal failure in 2 years, **I–L**, Cx43 heterogeneity score, 3; Cx43 intensity score, 2), segmental loss or thinning of Cx43 expression (**I**, **J**, white arrowheads) and segmental thickening of Cx43 expression (**I**, **J**, black arrows) were prominent. Scale bars, 50 μm (**A**, **C–E**, **G–I**, **K**, **L**) and 15 μm (**B**, **F**, **J**). sCr, serum creatinine.

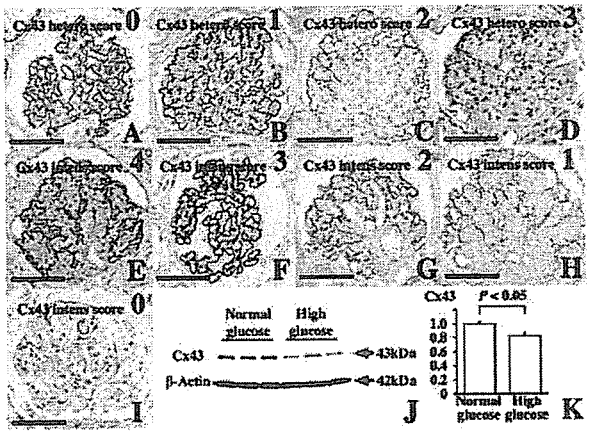

Fig. 2. Representative figures for Cx43 heterogeneity and Cx43 intensity score. Representative figures for Cx43 heterogeneity score (Cx43 hetero score, A–D): 0, without heterogeneity as in normal controls (**A**); 1, segmental heterogeneity, heterogeneity with conservation of more than half of glomerular linear Cx43 staining (**B**); 2, moderate heterogeneity, heterogeneity with less than half of glomerular linear Cx43 staining (**C**); 3, global heterogeneity, global heterogeneity with almost no preservation of linear Cx43 staining (**D**). Representative figures for Cx43 intensity score (Cx43 intens score, **E–I**): 4, highest expression, higher than normal controls (**E**); 3, high expression as observed in normal controls (**F**); 2, detectable expression (**G**); 1, only weak expression (**H**); 0, no expression detectable (**I**). Scale bars, 50 μm (**A–I**). Western blot analysis of Cx43 protein levels in cultured human podocytes grown in normal or high-glucose medium (**J**, **K**). Cx43 protein levels are reduced in podocytes cultured in high-glucose medium (25 mM) by 20% compared with cells grown in normal medium (5.5 mM) $n = 6$.

A level of $P < 0.05$ was considered statistically significant. Statistical analysis was performed using StatView (R) software package (Abacus Concepts, Berkeley, USA) and JUSE-package software version 2.42 (Union of Japanese Scientist and Engineers, Tokyo, Japan).

Results

Cx43 staining in normal controls showed a uniformly linear to a fine granular pattern along the glomerular basement membrane (GBM), indicating that Cx43 was almost exclusively expressed at podocytes within the glomeruli (Figure 1A and B). In diabetic nephropathy, Cx43 staining was still predominant in podocytes, but Cx43 staining in podocytes was down-regulated compared with normal controls (Figure 1E, F, I and J). In some patients, loss of uniformly linear Cx43 pattern in podocytes, i.e. segmental loss or thinning of Cx43 staining and thickened Cx43 staining in cytoplasm of podocytes, was observed (Figure 1I and J). Such Cx43 redistribution in podocytes was evaluated as 'Cx43 heterogeneity' by scoring from 0 (normal) to 3 (most advanced) (Figure 2A–D).

Magnitude of Cx43 intensity as scored from 0 (no signal) to 4 (highest expression, higher than normal controls) (Figure 2E–I) had no significant correlation with the degree of Cx43 heterogeneity (Figure 3E, Table 2). Cx43 intensity score correlated positively with creatinine clearance (Figure 3A) and inversely with serum creatinine (Figure 3B) at the time of renal biopsy. Cx43 heterogeneity score also had a weak correlation with creatinine clearance (Table 2). Although Cx43 intensity score did not show a significant association with the change in renal function (Table 2), Cx43 heterogeneity score closely correlated with the future decline in renal function, expressed as a monthly decline of inverse serum creatinine ($\Delta 1/sCr$) (Figure 3C, Table 2). Change in renal function correlated inversely with some of the previously reported promoters of diabetic nephropathy, such as the level of urinary protein at renal biopsy, systolic blood pressure, serum creatinine, BUN and urinary protein at follow-up [5] (Table 2). Cx43 intensity correlated positively with podocyte number per glomerular cross section, and inversely with systolic blood pressure at renal biopsy (Table 2). Cx43 heterogeneity correlated positively with the degree of urinary protein at renal biopsy, serum creatinine at renal biopsy and at follow-up, and BUN at follow-up (Figure 3D, Table 2).

To evaluate the mechanism of the altered Cx43 expression at podocytes in diabetic nephropathy, conditionally immortalized human podocyte cell line was cultured with a high-glucose (25 mM) or normal-glucose (5.5 mM) medium. High glucose decreased Cx43 expression by 20% compared with normal glucose (Figure 2J and K). These results show that, unlike murine podocytes, Cx43 is consistently and constitutively expressed at human podocytes, and that Cx43 expression can be decreased by high-glucose condition.

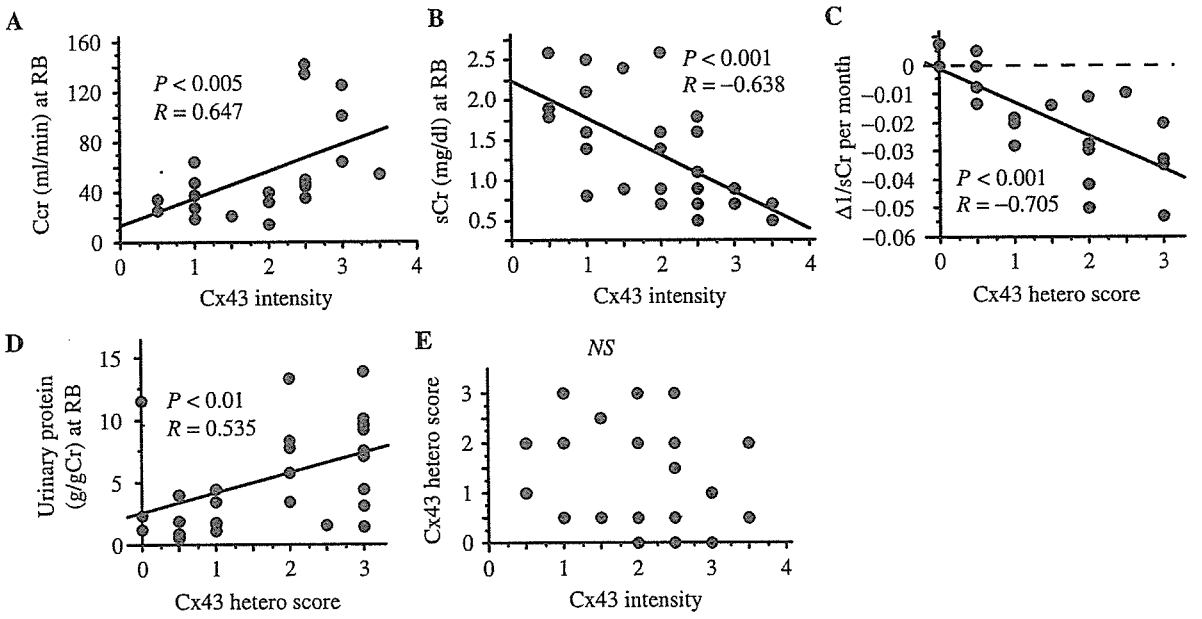

Fig. 3. Correlation of Cx43 intensity score and Cx43 heterogeneity score with renal function and proteinuria in patients with overt diabetic nephropathy. Cx43 intensity score significantly correlated positively with Ccr (**A**, $n = 21$, $R = 0.647$, $P < 0.005$), and inversely with serum creatinine (**B**, $n = 28$, $R = -0.638$, $P < 0.001$). Cx43 heterogeneity score correlated closely with the future decline in renal function (**C**, $n = 22$, $R = -0.705$, $P < 0.001$, observation period 23 ± 3 months), and positively with urinary protein at renal biopsy (**D**, $n = 27$, $R = 0.535$, $P < 0.01$). Cx43 intensity score did not significantly correlate with Cx43 heterogeneity score (**E**, $n = 28$). Ccr, creatinine clearance; sCr, serum creatinine; RB, renal biopsy.

Discussion

In the present study, we examined the staining pattern of Cx43 at glomerular podocytes in specimens obtained from normal controls and patients with overt diabetic nephropathy. In normal controls, Cx43 was expressed in a linear to a fine granular pattern along the GBM. In contrast, those with advanced diabetic nephropathy showed loss of uniformly linear Cx43 expression, which we termed gain of 'Cx43 heterogeneity'. Cx43 intensity correlated positively with renal function at renal biopsy, whereas the magnitude of podocyte damage assessed by Cx43 heterogeneity correlated well with the future decline in glomerular function.

Roles of podocyte injury in the progression of diabetic nephropathy remain to be elucidated. Anatomically, podocytes cover the entire surface of the GBM facing the urinary space in the Bowman's capsule [1]. 'Bare' GBM without podocytes represents a starting point for irreversible glomerular injury, since attachment of parietal epithelial cells to bare GBM progresses to glomerular sclerosis [1]. Decrease in podocyte number is observed in the early stage of nephropathy in diabetic patients [2] and in animal models of diabetic nephropathy [4]. Glomerular hypertrophy is another morphological feature in early diabetic nephropathy, which leads to the expansion of surface area of the GBM [5]. Since podocytes are incapable of regenerative replication post-natally and cannot be replaced by new cells [1], podocyte loss and glomerular hypertrophy in diabetic nephropathy must be compensated by migration and/or extension of cell body by the remaining podocytes to cover the GBM. In doing so, gap junction protein Cx43 in podocytes may play a role in intercellular communication [12].

In this study, Cx43 intensity in podocytes correlated positively with renal function at renal biopsy. There are not many reports on podocyte injury and renal function in diabetic nephropathy. Podocyte filtration slit length is related to the glomerular filtration rate (GFR) [13]. Podocyte cell number is also reported to be associated with GFR [3], but is still controversial. Here, we show that decrease in Cx43 intensity in podocytes can be useful in assessing podocyte injury in overt diabetic nephropathy. The findings that Cx43 intensity correlated positively with podocyte number per glomerular cross section, and inversely with systolic blood pressure at renal biopsy, support this notion (Table 2). Notably, Cx43 down-regulation (low Cx43 intensity) alone did not predict poor renal prognosis, but rather, Cx43 redistribution (high Cx43 heterogeneity) could predict. In normal human podocytes, Cx43 is localized strictly at cell–cell contact between podocytes [14]. Increased Cx43 heterogeneity, or Cx43 redistribution and down-regulation, at podocytes may impair intercellular communication, possibly leading to the loss of barrier function. The role of Cx43 redistribution in causing proteinuria should await further clarification.

Another possible role for podocyte injury in diabetic nephropathy may be alteration in the slit diaphragm [1]. Cx43 can directly bind to α- and β-tubulin [15], and to zona occludens-1 protein (ZO-1) [16]. Cx43 redistribution may influence slit diaphragm components through direct interaction with ZO-1 and tubulins in foot processes and major processes, respectively.

Table 2. Spearman's correlation coefficient for Cx43 intensity score, Cx43 heterogeneity score and change in renal function *vs* clinical parameters

	Cx43 heterogeneity score	Cx43 intensity score	Change in renal function (Δ1/sCr/month)
Cx43 heterogeneity score	1	−0.323	−0.705§
Cx43 intensity score	−0.323	1	0.253
Change in renal function (Δ1/sCr/month)	−0.705§	0.253	1
Age (years)	−0.095	−0.063	−0.025
sCr at renal biopsy (mg/dl)	0.459*	−0.638§	−0.255
BUN at renal biopsy (mg/dl)	0.306	−0.494†	0.023
HbA1c at renal biopsy (%)	−0.249	0.315	0.119
Ccr at renal biopsy (ml/min)	−0.402	0.647‡	0.235
Urinary protein at renal biopsy (g/gCr)	0.535†	−0.002	−0.606†
sCr at follow-up (mg/dl)	0.604†	−0.438*	−0.525*
BUN at follow-up (mg/dl)	0.686†	−0.542*	−0.605†
HbA1c at follow-up (%)	−0.161	0.428	0.000
Ccr at follow-up (ml/min)	−0.625	−1.000	0.500
Urinary protein at follow-up (g/gCr)	0.467	0.08	−0.599*
Podocyte/glomerulus (cells/glomerulus)	−0.020	0.456*	0.171
SBP at renal biopsy (mmHg)	0.296	−0.424*	−0.042
DBP at renal biopsy (mmHg)	0.203	−0.252	0.045
mBP at renal biopsy (mmHg)	0.189	−0.358	0.081
SBP at follow-up (mmHg)	0.412	−0.098	−0.593*
DBP at follow-up (mmHg)	−0.263	−0.041	0.262
mBP at follow-up (mmHg)	0.118	−0.095	−0.298

*$P < 0.05$, †$P < 0.01$, ‡$P < 0.005$, §$P < 0.001$.
sCr, serum creatinine; BUN, blood urea nitrogen; Ccr, creatinine clearance; SBP, systolic blood pressure; DBP, diastolic blood pressure; mBP, mean blood pressure.

Recent reports show that some unapposed connexons, called hemichannels, connect the intracellular and extracellular space [7]. Cx43 heterogeneity may indicate Cx43 hemichannel activation in podocytes, which may further lead to podocyte injury, as is the case with renal proximal tubule cells in ischaemic injury [17].

As we have shown in this study, persistent high glucose is a candidate mechanism for decrease in Cx43 intensity and the development of Cx43 heterogeneity in podocytes. High glucose is reported to reduce Cx43 expression in various other cell types [18]. Phosphorylation of Cx43, by kinases including protein kinase-C and mitogen-activated protein kinase [7], may also alter Cx43 expression and function, such as the regulation of trafficking, assembly, channel gating, internalization and degradation [7]. Although, there was no significant correlation between Cx43 heterogeneity and the level of glycaemic control in our study, Cx43 heterogeneity may result from the combined effects of factors aforementioned that were involved in the progression of diabetic nephropathy [19]. Mechanisms for Cx43 alteration in podocytes remain to be elucidated in the future.

Cx43 is abundantly expressed in myocardium but is also found in many other cell types [7]. Although Cx43 knockout mice seem to have normal kidney morphology [20], Cx43 expression in rodents and humans are quite different. In rodents, glomerular Cx43 expression is detected in the extraglomerular mesangium, mesangial cells and sparsely along the glomerular capillary wall in normal glomerulus [12]. In rodents, Cx43 becomes apparent only after podocyte injury [12]. In humans, however, Cx43 is most abundantly expressed in podocytes within the glomeruli [9,10]. Significance of Cx43 gene mutation in renal disease remains to be explored.

In summary, the findings of the present study indicate that alteration of podocyte Cx43 expression proceeds even after the establishment of overt diabetic nephropathy, being involved in further progression of the disease. Further analysis of the mechanism of Cx43 redistribution may elucidate the role of podocytes in the progression of overt diabetic nephropathy. Quantification of Cx43 staining may also be an easy and convenient way to assess podocyte damage and to predict future decline in renal function in diabetic patients with overt nephropathy.

Acknowledgements. The authors gratefully acknowledge Dr P.W. Mathieson for providing human podocytes, Dr K. Nagahama and Dr H. Nishiyama for discussion, Ms. J. Nakamura and Ms. S. Saito for technical assistance, and Ms. A. Sonoda and Ms. S. Doi for secretarial assistance. This work was supported in part by research grants from the Japanese Ministry of Education, Culture, Sports, Science and Technology, the Japanese Ministry of Health, Labour and Welfare, and Yamanouchi Foundation for Research on Metabolic Disorders.

Conflict of interest statement. None declared.

References

1. Pavenstt H, Kriz W, Kretzler M. Cell biology of the glomerular podocyte. *Physiol Rev* 2003; 83: 253–307
2. Pagtalunan ME, Miller PL, Jumping-Eagle S *et al.* Podocyte loss and progressive glomerular injury in type II diabetes. *J Clin Invest* 1997; 99: 342–348
3. Meyer TW, Bennett PH, Nelson RG. Podocyte number predicts long-term urinary albumin excretion in Pima Indians with type II diabetes and microalbuminuria. *Diabetologia* 1999; 42: 1341–1344
4. Suganami T, Mukoyama M, Mori K *et al.* Prevention and reversal of renal injury by leptin in a new mouse model of diabetic nephropathy. *FASEB J* 2005; 19: 127–129
5. Parving HH, Mauer M, Ritz E. Diabetic nephropathy. In: Brenner BM, ed. *The Kidney*, 7th edn, Vol. 2, Saunders, Philadelphia, USA: 2004; 1777–1818
6. Mauer SM, Goetz FC, McHugh LE *et al.* Long-term study of normal kidneys transplanted into patients with type I diabetes. *Diabetes* 1989; 38: 516–523
7. Saez JC, Berthoud VM, Branes MC, Martinez AD, Beyer EC. Plasma membrane channels formed by connexins: their regulation and functions. *Physiol Rev* 2003; 83: 1359–1400
8. Haefliger JA, Nicod P, Meda P. Contribution of connexins to the function of the vascular wall. *Cardiovasc Res* 2004; 62: 345–356
9. Hillis GS, Duthie LA, Mlynski R *et al.* The expression of connexin 43 in human kidney and cultured renal cells. *Nephron* 1997; 75: 458–463
10. Hillis GS, Duthie LA, Brown PA, Simpson JG, MacLeod AM, Haites NE. Upregulation and co-localization of connexin43 and cellular adhesion molecules in inflammatory renal disease. *J Pathol* 1997; 182: 373–379
11. Saleem MA, O'Hare MJ, Reiser J *et al.* A conditionally immortalized human podocyte cell line demonstrating nephrin and podocin expression. *J Am Soc Nephrol* 2002; 13: 630–638
12. Yaoita E, Yao J, Yoshida Y *et al.* Up-regulation of connexin43 in glomerular podocytes in response to injury. *Am J Pathol* 2002; 161: 1597–1606
13. Bjorn SF, Bangstad HJ, Hanssen KF *et al.* Glomerular epithelial foot processes and filtration slits in IDDM patients. *Diabetologia* 1995; 38: 1197–1204
14. Yaoita E, Miyazaki S, Yoshida Y *et al.* Connexin 43 expression of podocytes in human adult and fetal kidneys (abstract). *J Am Soc Nephrol* 2003; 14: A161
15. Giepmans BN, Verlaan I, Hengeveld T *et al.* Gap junction protein connexin-43 interacts directly with microtubules. *Curr Biol* 2001; 11: 1364–1368
16. Giepmans BN, Moolenaar WH. The gap junction protein connexin43 interacts with the second PDZ domain of the zona occludens-1 protein. *Curr Biol* 1998; 8: 931–934
17. Vergara L, Bao X, Cooper M, Bello-Reuss E, Reuss L. Gap-junctional hemichannels are activated by ATP depletion in human renal proximal tubule cells. *J Membr Biol* 2003; 196: 173–184
18. Sato T, Haimovici R, Kao R, Li AF, Roy S. Downregulation of connexin 43 expression by high glucose reduces gap junction activity in microvascular endothelial cells. *Diabetes* 2002; 51: 1565–1571
19. Rossing K, Christensen PK, Hovind P, Tarnow L, Rossing P, Parving HH. Progression of nephropathy in type 2 diabetic patients. *Kidney Int* 2004; 66: 1596–1605
20. Silverstein DM, Urban M, Gao Y, Mattoo TK, Spray DC, Rozental R. Renal morphology in connexin43 knockout mice. *Pediatr Nephrol* 2001; 16: 467–471

Received for publication: 18.8.05
Accepted in revised form: 18.4.06

Diabetologia (2006) 49:2514–2524
DOI 10.1007/s00125-006-0352-y

ARTICLE

Transgenic overexpression of brain natriuretic peptide prevents the progression of diabetic nephropathy in mice

H. Makino · M. Mukoyama · K. Mori · T. Suganami · M. Kasahara · K. Yahata · T. Nagae · H. Yokoi · K. Sawai · Y. Ogawa · S. Suga · Y. Yoshimasa · A. Sugawara · I. Tanaka · K. Nakao

Received: 21 October 2005 / Accepted: 15 May 2006 / Published online: 18 August 2006

Abstract
Aims/hypothesis Brain natriuretic peptide (BNP) is a potent vasorelaxing and natriuretic peptide that is secreted from the heart and has cardioprotective properties. We have previously generated hypotensive transgenic mice (BNP-Tg mice) that overproduce BNP in the liver, which is released into the circulation. Using this animal model, we successfully demonstrated the amelioration of renal injury after renal ablation and in proliferative glomerulonephritis. Glomerular hyperfiltration is an early haemodynamic derangement, representing one of the key mechanisms of the pathogenesis of diabetic nephropathy. Based on the suggested involvement of increased endogenous natriuretic peptides, the aim of this study was to investigate their role in the development and progression of diabetic nephropathy.
Materials and methods We evaluated the progression of renal injury and fibrogenesis in BNP-Tg mice with diabetes induced by streptozotocin. We also investigated the effect of BNP on high glucose-induced signalling abnormalities in mesangial cells.
Results After induction of diabetes, control mice exhibited progressively increased urinary albumin excretion with impaired renal function, whereas these changes were significantly ameliorated in BNP-Tg mice. Notably, diabetic BNP-Tg mice revealed minimal mesangial fibrogenesis with virtually no glomerular hypertrophy. Glomerular upregulation of extracellular signal-regulated kinase, TGF-β and extracellular matrix proteins was also significantly inhibited in diabetic BNP-Tg mice. In cultured mesangial cells, activation of the above cascade under high glucose was abrogated by the addition of BNP.
Conclusions/interpretation Chronic excess of BNP prevents glomerular injury in the setting of diabetes, suggesting that renoprotective effects of natriuretic peptides may be therapeutically applicable in preventing the progression of diabetic nephropathy.

Keywords Diabetic nephropathy · Extracellular matrix · Glomerular hyperfiltration · Natriuretic peptide · Transforming growth factor-β · Transgenic mice

Abbreviations

ANP	atrial natriuretic peptide
BNP	brain natriuretic peptide
cGMP	guanosine 3′,5′-cyclic monophosphate
CNP	C-type natriuretic peptide
ERK	extracellular signal-regulated kinase
GC	guanylyl cyclase
MAPK	mitogen-activated protein kinase
PKC	protein kinase C
PMA	phorbol 12-myristate 13-acetate
Tg	transgenic

Introduction

Among diabetic complications, an increasing prevalence of nephropathy is one of the most intractable and serious problems worldwide [1]. Diabetic nephropathy is the leading cause of end-stage renal disease in many countries,

H. Makino · M. Mukoyama (✉) · K. Mori · T. Suganami · M. Kasahara · K. Yahata · T. Nagae · H. Yokoi · K. Sawai · Y. Ogawa · A. Sugawara · I. Tanaka · K. Nakao
Department of Medicine and Clinical Science,
Kyoto University Graduate School of Medicine,
54 Shogoin Kawahara-cho,
Sakyo-ku, Kyoto 606-8507, Japan
e-mail: muko@kuhp.kyoto-u.ac.jp

H. Makino · S. Suga · Y. Yoshimasa
National Cardiovascular Center Research Institute,
Suita 565-8565, Japan

and effective therapy to prevent progression at advanced stages remains unsatisfactory [1–3]. Hyperglycaemia is a necessary precondition for the development of diabetic renal lesions [4, 5], while systemic hypertension is an equally important aggravating factor of the disease [6]. Mechanisms including glomerular hypertension with hyperfiltration, renin–angiotensin system (RAS) activation, increased oxidative stress and advanced glycation end-products, activation of the protein kinase C (PKC) and mitogen-activated protein kinase (MAPK) pathways, growth factors and cytokines such as TGF-β, and genetic susceptibility have been identified as important deteriorating factors [2, 7, 8], but the precise mechanisms involved in the progression of diabetic renal injury remain elusive.

The natriuretic peptide family, consisting of atrial natriuretic peptide (ANP), brain natriuretic peptide (BNP) and C-type natriuretic peptide (CNP) [9], possesses potent diuretic, natriuretic and vasorelaxing properties, thereby regulating blood pressure, body fluid homeostasis and cardiorenal function [10, 11]. ANP and BNP are secreted predominantly by the cardiac atrium and ventricle, respectively, in response to volume expansion and ventricular wall stress [9, 11]. Increased cardiac secretion of BNP, as well as ANP, has been demonstrated in patients with cardiovascular diseases such as congestive heart failure, hypertension and renal failure, serving as one of the compensatory mechanisms against disease progression [11, 12]. ANP and BNP share the same receptor, a particulate guanylyl cyclase (GC)-coupled receptor, or GC-A, and exert almost identical actions [13]. The peptides are thought to function, in general, to antagonise the RAS both systemically and locally [9].

Elevated plasma levels of ANP and BNP are reported in patients with diabetic nephropathy [14–16]. Plasma BNP and pro-BNP also serve as powerful risk markers for cardiovascular disease in patients with diabetic nephropathy [17]. Glomerular hyperfiltration, one of the key mechanisms of the pathogenesis of diabetic nephropathy [2], is an early haemodynamic derangement observed in diabetes, and the involvement of increased endogenous natriuretic peptides has been suggested. Indeed, in experimental diabetic nephropathy, the blockade of elevated plasma ANP attenuated glomerular hyperfiltration and urinary albumin excretion [18, 19]. In addition, acute infusion of ANP augmented urinary albumin excretion in diabetic patients with nephropathy [16]. These observations suggest that natriuretic peptides may play a causative role in glomerular hyperfiltration and diabetic glomerular injury.

Conversely, several reports have shown potential renoprotective effects of natriuretic peptides on various nephropathies. Administration of ANP exerted beneficial effects in experimental and clinical acute renal failure [20, 21]. We generated hypotensive transgenic mice overexpressing the mouse gene encoding BNP (*Nppb*) in the liver (BNP-Tg mice), which showed more than a 100-fold increase in plasma BNP and constitutive elevation of urinary guanosine 3′,5′-cyclic monophosphate (cGMP) levels [22]. Using this animal model, we successfully demonstrated amelioration of renal injury after renal ablation [23] and in proliferative glomerulonephritis [24]. However, the long-term effects of increased natriuretic peptides on diabetic renal injury remain unknown. The aim of the present study was to investigate the effects of a chronic excess of BNP on diabetic renal injury using streptozotocin-induced diabetes in BNP-Tg mice. We also studied the actions of BNP on cultured mesangial cells in the presence of high glucose.

Materials and methods

Animals All animal experiments were conducted in accordance with our institutional guidelines for animal research. Generation of BNP-Tg mice (line 55) harbouring 20 copies of the transgene under the control of the human serum amyloid P component promoter has been reported elsewhere [22–24]. This promoter is active only in the liver after birth [22]. BNP-Tg mice and their littermates, C57BL/6J non-transgenic mice (non-Tg mice), were 10 weeks of age at the beginning of this study. Mice were fed on standard chow (CE-2 containing 0.5% NaCl; Clea Japan, Tokyo, Japan) and given free access to water. We maintained the animals under alternating 12-h cycles of light and dark.

Induction of diabetes Diabetes was induced in mice by daily intraperitoneal injection of streptozotocin (70 mg/kg body weight, for 4-7 days) (Sigma, St Louis, MO, USA) in citrate buffer until the blood glucose level was raised to >16.7 mmol/l [25]. Control mice received citrate buffer only. Blood glucose was measured in tail vein blood using the *o*-toluidine method (Sigma kit) [25] under non-fasted conditions. Blood pressure was measured every 4 weeks by the indirect tail-cuff method [23]. Urine specimens (24 h) were obtained from each mouse every 4 weeks for measurement of creatinine and albumin [24]. Urinary albumin excretion was assayed with a murine albumin ELISA kit (Exocell, Philadelphia, PA, USA). Urinary and serum creatinine levels were measured using an enzymatic method (SRL, Tokyo, Japan) [24]. A subgroup of the diabetic non-Tg mice were administered hydralazine [23]; mice were given drinking water containing 60 mg/l hydralazine hydrochloride (Sigma) from 1 week after the induction of diabetes. Mice were killed after 16 weeks of diabetes under ether anaesthesia, and samples were collected for histological and biochemical analyses.

Renal histology and morphometric analysis Kidney sections were fixed by immersion in Carnoy's solution, followed by 4% buffered formaldehyde, and embedded in paraffin. Sections (2 μm thick) were stained with periodic acid–Schiff and examined by light microscopy. Measurement of the glomerular cross-sectional area and the mesangial area of 30 glomeruli randomly selected in each mouse by scanning of the outer cortex was performed with a computer-aided manipulator (KS-400; Carl Zeiss Vision, Munich, Germany) [23, 24].

Immunohistochemistry For immunohistochemical study of TGF-β, the kidney sections embedded in Optimal Cutting Temperature (OCT) compound (Sakura Finetechnical, Tokyo, Japan) were snap frozen in acetone/dry ice, and 4-μm-thick cryostat sections were fixed in acetone [23]. The sections were washed with phosphate-buffered saline, and treated with 0.9% H_2O_2 in methanol for 30 min to quench endogenous peroxidase activity. The specimens were incubated overnight at 4°C with rabbit anti-mouse TGF-β antibody (Santa Cruz Biotechnology, Santa Cruz, CA, USA). After incubation with biotin-conjugated second antibody, the specimens were processed by use of an avidin–biotin–peroxidase complex kit (Vector, Burlingame, CA, USA) and developed with 3,3'-diaminobenzidine tetrahydrochloride (Kanto Chemical, Tokyo, Japan).

Cell culture Mesangial cells were established from glomeruli isolated from 10-week-old male Sprague–Dawley rats using a differential sieving method [25, 26] and used at passages 7–10. Mesangial cells were identified by immunofluorescence techniques [26]. Cells were grown in DMEM (Gibco BRL, Grand Island, NY, USA) containing 20% FCS (Sanko Junyaku, Tokyo, Japan). As the cells reached 80% confluence, they were grown in DMEM containing 10% FCS supplemented with 5.6 mmol/l glucose (normal glucose), 25 mmol/l glucose (high glucose), or 5.6 mmol/l glucose plus 19.4 mmol/l mannitol (as an osmotic control) for 5 days. After this time, the medium was changed to DMEM containing 0.2% FCS supplemented with 5.6 mmol/l glucose, 25 mmol/l glucose, or 5.6 mmol/l glucose plus 19.4 mmol/l mannitol for 24 h. Then, in the presence or absence of rat BNP (100 nmol/l) (Peptide Institute, Osaka, Japan) or 8-bromo-cGMP (1 mmol/l) (Sigma), the cells were further incubated for 24 h. Phorbol 12-myristate 13-acetate (100 nmol/l) (PMA; Sigma) was used for the activation of PKC [26].

Northern blot analysis Total RNA was extracted from whole kidney and mesangial cells by the acid guanidinium–phenol–chloroform method and used for northern blot analysis as described previously [24, 25]. In brief, 25 μg of total RNA was electrophoresed on 1.1% agarose gels containing 2.2 mol/l formaldehyde, and RNA was transferred onto nylon membrane filters. The cDNA fragments corresponding to genes for rat TGF-β_1 (*Tgfb1*, nt 1142–1546), rat fibronectin (*Fn1*, nt 619–1082), mouse α1(IV) collagen (*Col4a1*, nt 5808–6165) and mouse TGF-β_1 (*Tgfb1*, nt 1141–1549), which were prepared by RT-PCR using rat and mouse kidney mRNA, were used as probes. The filter was hybridised with radiolabelled probes and autoradiography was performed using a BAS-2500 bioimaging analyser (Fuji Photo film, Tokyo, Japan). The filters were rehybridised with human *GAPDH* cDNA probe for normalisation.

Western blot analysis Whole-kidney tissues and mesangial cells were lysed on ice in lysis buffer containing 1 mol/l Tris–HCl (pH 7.5), 12 mmol/l β-glycerophosphate, 0.1 mol/l EGTA, 1 mmol/l pyrophosphate, 5 mmol/l NaF, 10 mg/ml aprotinin, 2 mmol/l dithiothreitol, 1 mmol/l sodium orthovanadate, 1 mmol/l phenylmethylsulfonyl fluoride, and 1% Triton X-100 [24]. The lysates were centrifuged at 15,000 ×*g* for 20 min at 4°C, and supernatants mixed with Laemmli's sample buffer (40 μg protein/lane) were separated by 12.5% SDS-PAGE

Table 1 Characteristics of control and diabetic mice at 16 weeks

	Control		Diabetes	
	non-Tg (*n*=5)	BNP-Tg (*n*=8)	non-Tg (*n*=10)	BNP-Tg (*n*=10)
Blood glucose (mmol/l)	8.5±1.7	9.8±1.0	27.2±1.8[b]	31.1±0.9[c]
Systolic blood pressure (mmHg)	112±3	90±2[b]	108±2	92±2[d]
Body weight (g)	31.9±1.2	34.4±1.5	27.4±1.0[b]	31.6±0.5[c]
Kidney weight (g)	0.20±0.01	0.21±0.01	0.22±0.01	0.20±0.01
Kidney/body weight (%)	6.30±0.46	5.93±0.30	7.96±0.47[a]	6.37±0.28[d]

Values are expressed as means±SEM
[a] $p<0.05$ vs control non-Tg mice
[b] $p<0.005$ vs control non-Tg mice
[c] $p<0.005$ vs control BNP-Tg mice
[d] $p<0.05$ vs. diabetic non-Tg mice

and electrophoretically transferred onto Immobilon filters. The filters were incubated with antibodies against total extracellular signal-regulated kinase (ERK)-1/2 or phosphorylated ERK-1/2 (New England Biolabs, Boston, MA, USA) for 2 h at room temperature, and immunoblots were developed with horseradish peroxidase-conjugated donkey anti-rabbit IgG (Bio-Rad, Richmond, CA, USA) and a chemiluminescence kit (ECL One Plus; Amersham, Arlington Heights, IL, USA).

Statistical analysis Data are expressed as means±SEM. Statistical analysis was performed by ANOVA followed by Scheffe's test. A p value of <0.05 was considered statistically significant.

Results

Characteristics of diabetic mice At baseline, there was no significant difference between BNP-Tg and non-Tg mice in terms of blood glucose levels (9.1±0.4 vs 8.5±1.1 mmol/l, n=10 per group), body weight or kidney weight (data not shown). After induction of diabetes, both BNP-Tg and non-Tg mice exhibited sustained hyperglycaemia, with no significant difference in blood glucose levels between them (Table 1). At baseline, the blood pressure of the BNP-Tg mice was 15–20 mmHg lower than that of the non-Tg mice, as observed previously [23, 24], and remained significantly lower during the study (Table 1). There were no significant blood pressure changes in the two groups following the induction of diabetes. At 16 weeks, diabetic non-Tg mice showed renal hypertrophy, as indicated by an increase in kidney weight per body weight, whereas BNP-Tg mice did not (Table 1).

Renal function and proteinuria of diabetic mice To evaluate the functional alterations in the kidneys of diabetic mice, we examined urinary albumin excretion and serum creatinine and urea nitrogen levels, together with calculated creatinine clearance. At baseline, there were no significant differences in these parameters between control non-Tg and control BNP-Tg mice (Fig. 1a; see [23]). After induction of diabetes, urinary albumin excretion of diabetic non-Tg mice markedly increased by 4 weeks, peaked at 12 weeks, and remained significantly elevated until 16 weeks (23.4± 6.4, 142.7±33.1, 264.3±46.5, 290.3±55.0, and 181.5± 22.7 μg/day at 0, 4, 8, 12 and 16 weeks, respectively, n=10). In diabetic BNP-Tg mice, on the other hand, the increase in urinary albumin excretion was much attenuated and significantly milder than that observed in diabetic non-Tg mice at 8, 12 and 16 weeks (31.1±6.6, 100.8±22.6, 136.6±24.5, 144.1±18.6, and 120.6±19.2 μg/day at 0, 4, 8, 12 and 16 weeks, respectively, n=10) (Fig. 1a). Urinary albumin excretion adjusted for creatinine was also significantly lower (~50%) in diabetic BNP-Tg mice than in diabetic non-Tg mice and was not significantly different from that seen in control non-Tg mice (Fig. 1b).

After 16 weeks of diabetes, non-Tg mice exhibited significantly increased serum creatinine and urea nitrogen levels, together with reduced creatinine clearance (Table 2). In contrast, these parameters were not significantly different from controls in diabetic BNP-Tg mice (Table 2). Thus, functional impairment became manifest at the chronic

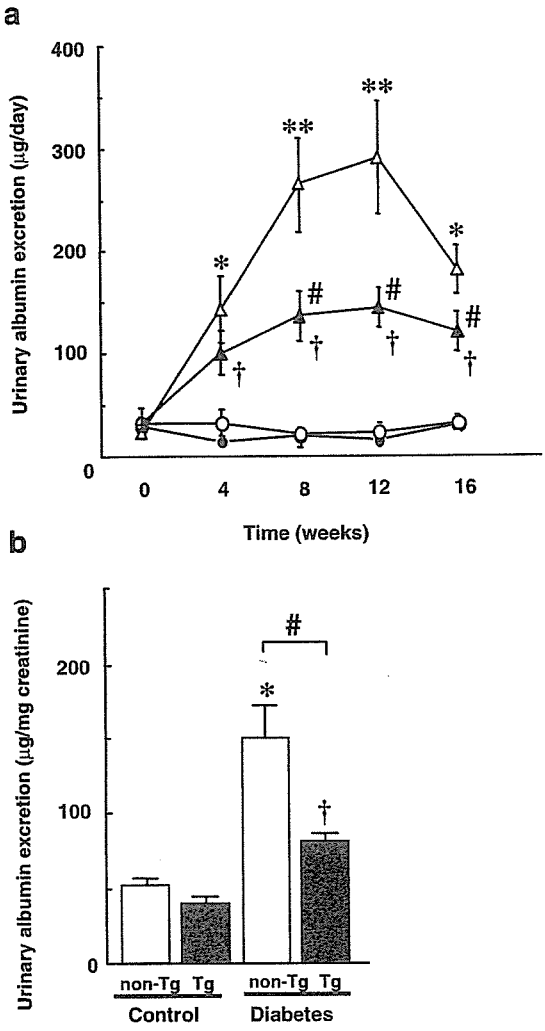

Fig. 1 **a** Daily urinary albumin excretion of control and diabetic mice at 0, 4, 8, 12 and 16 weeks after induction of diabetes. *Open circles*, control non-Tg mice (n=5); *closed circles*, control BNP-Tg mice (n=8); *open triangles*, diabetic non-Tg mice (n=10); *closed triangles*, diabetic BNP-Tg mice (n=10). **b** Urinary albumin excretion normalised to creatinine at 16 weeks. *p<0.05, **p<0.02 vs control non-Tg mice; †p<0.05 vs control BNP-Tg mice; #p< 0.05 vs diabetic non-Tg mice

Table 2 Renal function of control and diabetic mice at 16 weeks

Parameter	Control		Diabetes	
	non-Tg (n=5)	BNP-Tg (n=8)	non-Tg (n=10)	BNP-Tg (n=10)
Serum creatinine (μmol/l)	8.8±0.9	9.7±1.8	18.6±1.8[b]	12.4±0.9[c]
Blood urea nitrogen (mmol/l)	11.4±0.9	11.2±0.9	16.8±1.4[a]	14.6±1.6
Creatinine clearance (ml/min)	0.56±0.11	0.57±0.10	0.30±0.05[a]	0.54±0.06[c]

Values are expressed as means±SEM
[a] $p< 0.05$ vs control non-Tg mice
[b] $p< 0.02$ vs control non-Tg mice
[c] $p< 0.05$ vs diabetic non-Tg mice

phase in diabetic non-Tg mice, whereas renal function was well preserved in diabetic BNP-Tg mice.

Renal histology of diabetic mice We examined renal histological changes in diabetic non-Tg and BNP-Tg mice 16 weeks after induction of diabetes (Fig. 2). Compared with control (Fig. 2a), diabetic non-Tg mice showed

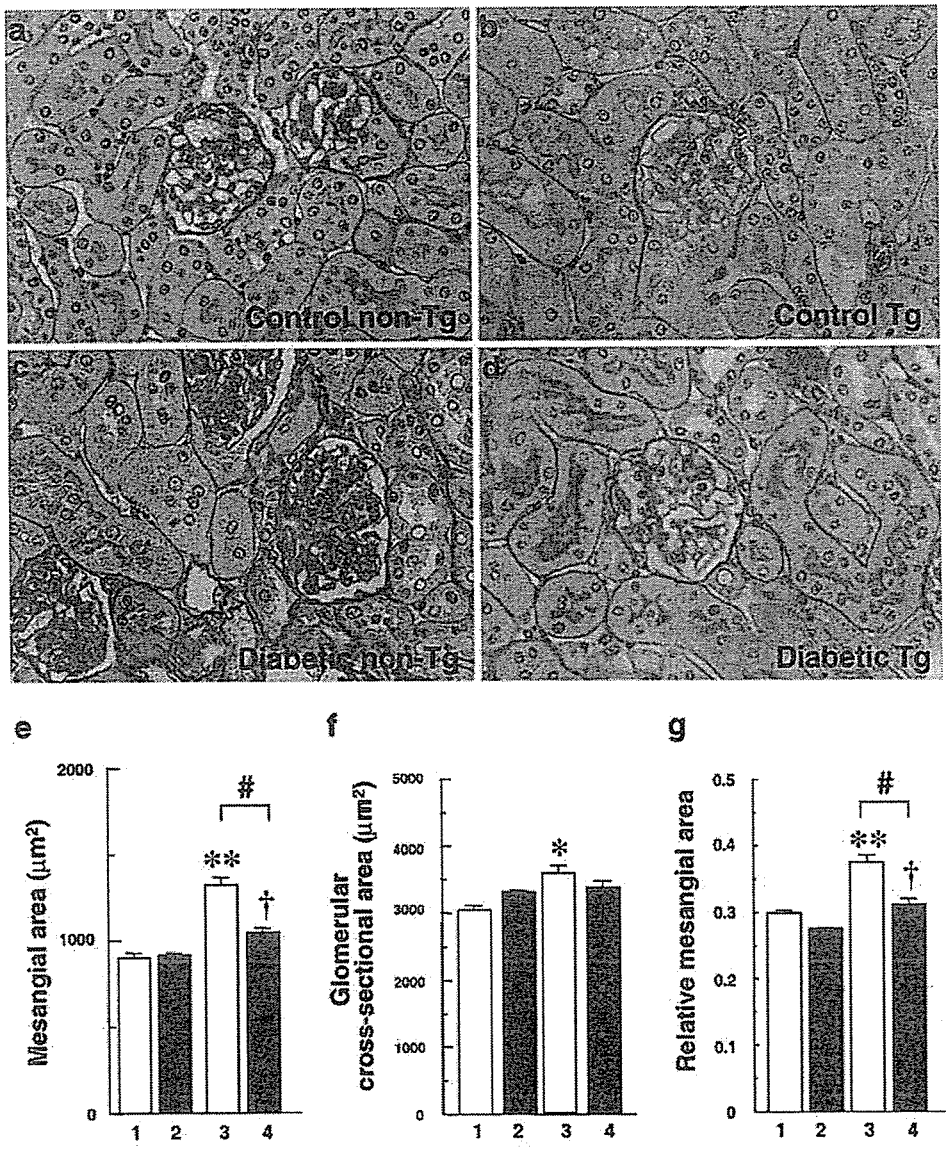

Fig. 2 Glomerular histology of diabetic mice at 16 weeks after induction of diabetes. Representative glomeruli from control non-Tg (**a**), control BNP-Tg (**b**), diabetic non-Tg (**c**), and diabetic BNP-Tg (**d**) mice are shown. Periodic acid–Schiff stain; magnification: ×400. Glomerular mesangial area (**e**), glomerular cross-sectional area (**f**) and relative mesangial area (**g**) in control and diabetic mice at 16 weeks. 1, control non-Tg mice (n=5); 2, control BNP-Tg mice (n=8); 3, diabetic non-Tg mice (n=10); 4, diabetic BNP-Tg mice (n=10) . Values are expressed as means±SEM. $^{*}p<0.05$, $^{**}p<0.01$ vs control non-Tg mice; $^{\dagger}p<0.05$ vs control BNP-Tg mice; $^{\#}p<0.01$ vs diabetic non-Tg mice

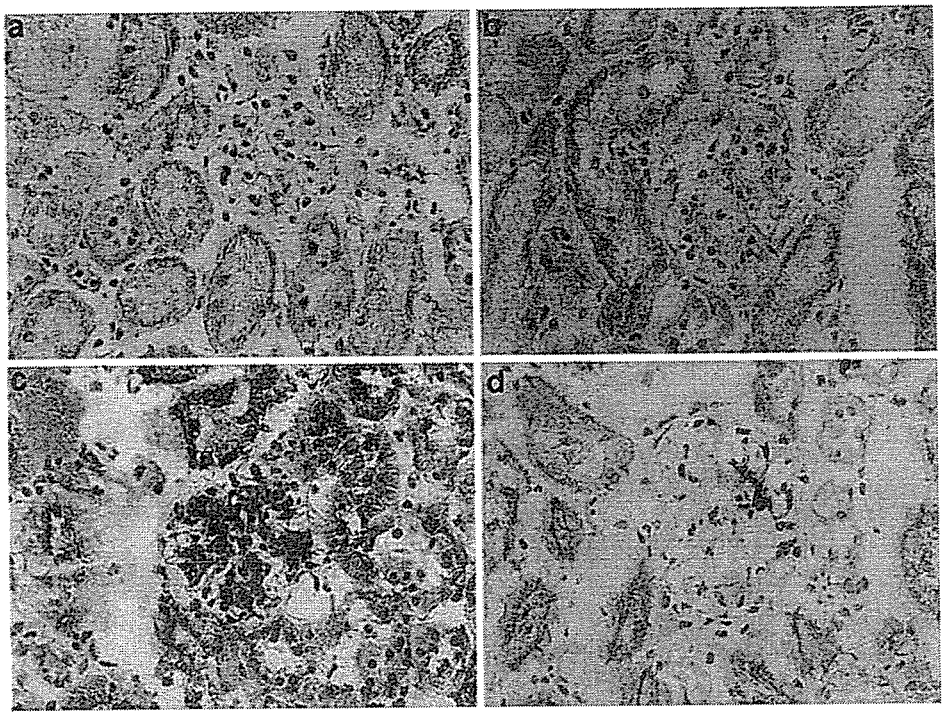

Fig. 3 Immunohistochemistry of TGF-β in control and diabetic mouse kidney at 16 weeks after induction of diabetes. Representative glomeruli from control non-Tg (**a**), control BNP-Tg (**b**), diabetic non-Tg (**c**), and diabetic BNP-Tg (**d**) mice are shown. Magnification: ×400

marked mesangial expansion and glomerular hypertrophy, along with partial tubular atrophy (Fig. 2c). In contrast, renal histology of diabetic BNP-Tg mice revealed only minimal glomerular hypertrophy and mesangial expansion with almost intact tubules (Fig. 2d), and was virtually indistinguishable from that of control BNP-Tg mice (Fig. 2b). Quantitative analysis revealed that the increase in mesangial area was marked in diabetic non-Tg mice, whereas this increase was significantly suppressed in diabetic BNP-Tg mice (1,328±58 vs. 1,037±21 μm^2, $p<0.01$, $n=10$ per group) (Fig. 2e). Glomerular hypertrophy was evident in diabetic non-Tg mice compared with control non-Tg mice (3,574±107 vs 3,048±66 μm^2, $p<0.05$), but was not apparent in BNP-Tg mice (3,378±103 vs 3,313± 30 μm^2 for diabetic vs control, respectively) (Fig. 2f). Accordingly, the increase in the relative mesangial area (mesangial area per glomerulus) was significantly blunted in diabetic BNP-Tg mice (Fig. 2g). Among the control mice, the mean glomerular area was slightly larger in the BNP-Tg mice than the non-Tg mice, but this difference was not statistically significant (Fig. 2f). These results indicate that the renal histological changes characteristic of diabetic nephropathy were prevented to a great extent in BNP-Tg mice.

Renal TGF-β1 expression The upregulation of TGF-β is postulated to play a pivotal role in facilitating extracellular matrix accumulation and subsequent glomerulosclerosis in diabetic glomerular injury [27, 28]. We therefore examined renal expression of the genes for TGF-β_1 (*Tgfb1*) and α1 (IV) collagen (*Col4a1*) in diabetic mice. By immunohistochemistry, we found that levels of TGF-β were markedly elevated in diabetic non-Tg mice (Fig. 3c) compared with control non-Tg mice (Fig. 3a), especially in the mesangial area. In diabetic BNP-Tg mice, on the other hand, this increase was significantly attenuated (Fig. 3d vs Fig. 3b). Likewise, northern blot analyses for *Tgfb1* and *Col4a1* revealed 3.5- to 4-fold increases in diabetic non-Tg mice compared with control ($p<0.05$, $n=7$) (Fig. 4a,b), whereas this upregulation was significantly reduced in diabetic BNP-Tg mice (1.3-fold increase relative to control BNP-Tg mice, $p<0.05$ vs diabetic non-Tg mice) (Fig. 4b). Thus, glomerular activation of the TGF-β-extracellular matrix protein cascade was significantly inhibited in diabetic BNP-Tg mice.

Renal ERK activation Accumulating evidence indicates that activation of the ERK/MAPK signalling pathway plays a key role in the induction of *Tgfb1* and extracellular matrix accumulation in diabetic nephropathy [29–31]. To address the mechanisms by which *Tgfb1* and matrix gene expression was inhibited in BNP-Tg mice, we investigated the phosphorylation of ERK in the kidney. Although ERK phosphorylation was minimal in the kidney tissues of both non-Tg and BNP-Tg mice under basal conditions, we found that levels of phosphorylated ERK were significantly increased in kidneys of diabetic mice (Fig. 5a). Importantly, phosphorylation of ERK in vivo was significantly lower in kidneys of diabetic BNP-Tg mice relative to diabetic non-Tg mice (Fig. 5b).

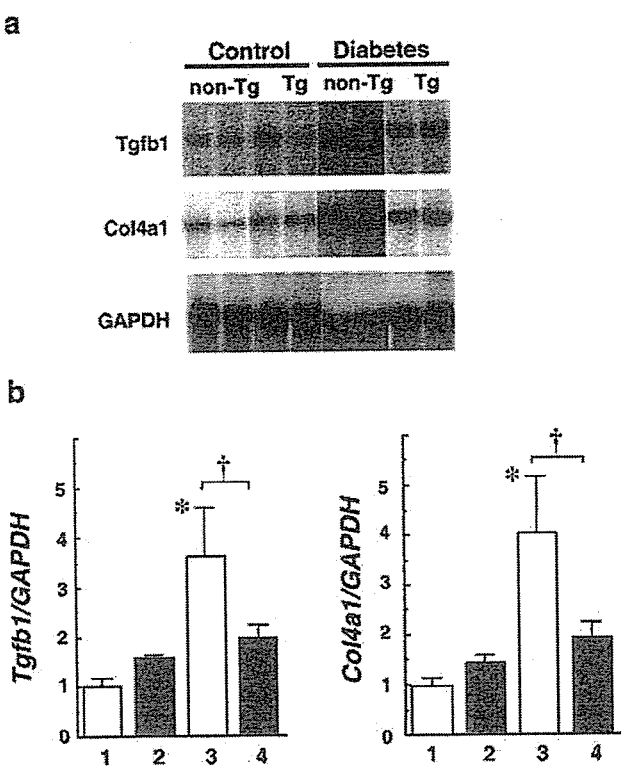

Fig. 4 Representative northern blots for *Tgfb1* and *Col4a1* mRNA expression (**a**) and their quantitative analysis (**b**) in kidney of control and diabetic mice at 16 weeks after induction of diabetes. 1, control non-Tg mice (n=4); 2, control BNP-Tg mice (n=4); 3, diabetic non-Tg mice (n=7); 4, diabetic BNP-Tg mice (n=7). Values are expressed as means±SEM. *p<0.05 vs control non-Tg mice. †p<0.05

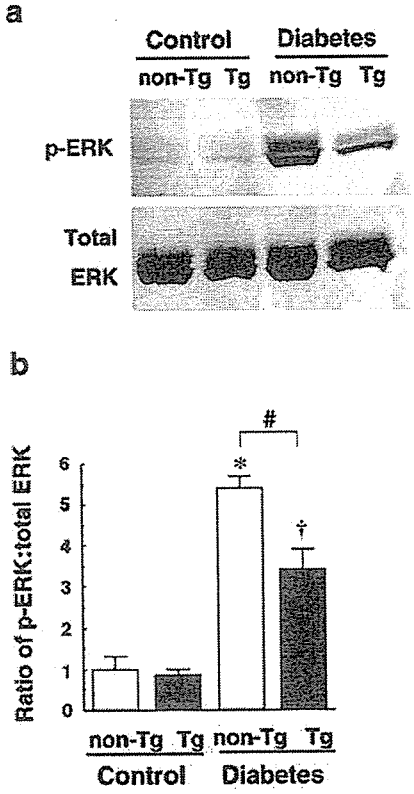

Fig. 5 ERK phosphorylation in the kidney of diabetic mice. Representative western blots of phosphorylated ERK-1/2 and total ERK-1/2 at 16 weeks after induction of diabetes (**a**) and quantitative analysis of phospho-ERK:total ERK (**b**). Values are expressed as means±SEM for n=4 in each group. *p<0.01 vs control non-Tg mice; †p<0.01 vs control BNP-Tg mice. #p<0.01

Effects of hydralazine administration Analyses thus far have suggested that a chronic excess of BNP prevents the progression of diabetic renal injury. Systemic blood pressure reduction is crucial to retard the progression of renal and vascular complications in diabetes [6, 32]. In order to explore whether the beneficial effects observed in BNP-Tg mice were the result of systemic hypotension, we studied the effect of hydralazine administration in diabetic non-Tg mice. Despite an effective reduction in systemic blood pressure to a level comparable to that in diabetic BNP-Tg mice (Fig. 6a), this treatment failed to prevent the increase in albuminuria (Fig. 6b) or to alleviate renal histological changes (data not shown). These results indicate that systemic hypotension in BNP-Tg mice does not play an important role in the renoprotective effects observed.

Effects of BNP in cultured mesangial cells under high glucose We next addressed the direct actions exerted by BNP using cultured mesangial cells under high glucose conditions. First, we investigated the effects of BNP on the expression of *Tgfb1* and the gene encoding its downstream effector, fibronectin. High glucose conditions significantly augmented *Tgfb1* and *Fn1* mRNA expression (1.8-fold and 1.5-fold of control [normal glucose, no BNP], respectively) (Fig. 7a,b). This effect was not simply due to high osmotic conditions, because an osmotic control with mannitol had no effect on *Tgfb1* mRNA expression (1.7-fold of control with high glucose vs 1.1-fold with mannitol, p<0.05) (Fig. 7c). This upregulation of *Tgfb1* and *Fn1* under high glucose conditions was effectively abolished by the addition of BNP (1.2-fold and 1.0-fold of control, respectively, p<0.01), or with a membrane-permeable analogue of cGMP (1.1-fold and 0.9-fold of control, respectively, p<0.01) (Fig. 7a,b).

We further examined the effects of BNP and cGMP on ERK phosphorylation of mesangial cells under high glucose conditions. High glucose-induced ERK phosphorylation in mesangial cells was significantly inhibited by the addition of BNP or cGMP (Fig. 8a). Moreover, BNP and cGMP effectively prevented ERK phosphorylation induced by PKC activation with PMA (Fig. 8b). Taken together, these results suggest that BNP inhibited PKC-ERK pathway activation and subsequent matrix gene activation, at least in part, locally in the mesangium in vivo, thereby leading to the amelioration of diabetic renal injury.

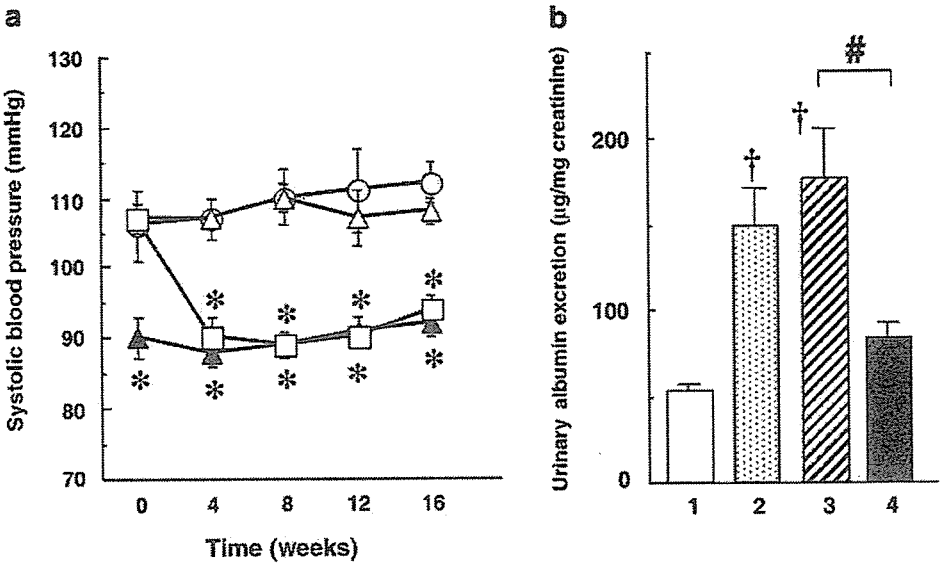

Fig. 6 **a** Effects of hydralazine administration on systolic blood pressure. *Open circles*, control non-Tg mice (n=5); *open triangles*, diabetic non-Tg mice (n=10); *closed triangles*, diabetic BNP-Tg mice (n=10); *open squares*, hydralazine-treated diabetic non-Tg mice (n=7). *p<0.005 vs diabetic non-Tg mice. **b** Urinary albumin excretion normalised to creatinine at 16 weeks. 1, control non-Tg mice; 2, diabetic non-Tg mice; 3, hydralazine-treated diabetic non-Tg mice; 4, diabetic BNP-Tg mice. †p<0.02 vs control non-Tg mice; #p<0.05

Discussion

Previous reports have suggested that increased natriuretic peptides may affect the course of diabetic nephropathy. Acute inhibition of elevated plasma ANP decreased hyperfiltration and albuminuria in experimental models [18, 19]. In patients with early-stage type 1 diabetes, ANP concentration was correlated with glomerular filtration rate [33]. Furthermore, acute ANP infusion increased the glomerular filtration rate, filtration fraction and albuminuria [34]. These studies investigated early haemodynamic abnormalities or only short-term effects of ANP (within several hours). Thus, the aim of this study was to assess the long-term effects of natriuretic peptides on glomerular function and histology. In order to address these issues, we investigated the effects of a chronic excess of BNP on the progression of diabetic nephropathy using BNP-Tg mice.

In this study, we demonstrate that transgenic overexpression of BNP prevents the progression of diabetic nephropathy in mice. In diabetic BNP-Tg mice, the accumulation of mesangial matrix was only minimal, with virtually no glomerular hypertrophy, in contrast to the histology of diabetic non-Tg mice (Fig. 2). Consistent with such histological amelioration, albuminuria was significantly attenuated in BNP-Tg mice, and renal function was well preserved (Fig. 1, Table 2). Although absolute creatinine values may be less accurate than those measured by HPLC, assessment of renal function in these groups should be valid considering the changes in serum creatinine essentially paralleled those in urea nitrogen (Table 2). These findings provide the first evidence that a chronic excess of BNP prevents the kidney from developing diabetic renal injury. We also demonstrated that the upregulation of *Tgfb* expression and protein levels in diabetic kidneys were markedly inhibited in BNP-Tg mice (Figs 3, 4). Considering a pathogenic role for TGF-β in cellular dysfunction, fibrogenesis and glomerular hypertrophy in diabetes [3, 28, 35], it is conceivable that the inhibition of renal TGF-β system activation contributed significantly to the observed protective effects of BNP from diabetic renal injury. Although the effect of BNP on glomerular haemodynamics was not investigated, it may be possible that the chronic excess of BNP lessened glomerular hypertension by inhibiting the RAS and TGF-β system tonically. It has been shown that combined inhibition of both angiotensin-converting enzyme and neutral endopeptidase, which potentiates ANP and BNP, results in lower glomerular capillary pressure than the former alone in subtotally nephrectomised rats [36].

There is no doubt that tight blood pressure control is important for retarding or preventing the progression of diabetic renal injury [6, 32]. Clearly, the diabetic BNP-Tg mice showed lower blood pressure. Although systemic blood pressure reduction with hydralazine treatment failed to alleviate nephropathy in diabetic non-Tg mice (Fig. 6), precise blood pressure profiles should have been different between the two hypotensive groups. We therefore cannot exclude the possibility that low blood pressure could account for the observed renoprotective effect in BNP-Tg mice.

ERK plays a pivotal role in activating mesangial TGF-β expression/signalling and extracellular matrix accumulation [29, 30]. We clearly show that ERK activation in the kidney tissue was significantly attenuated in BNP-Tg mice (Fig. 5).

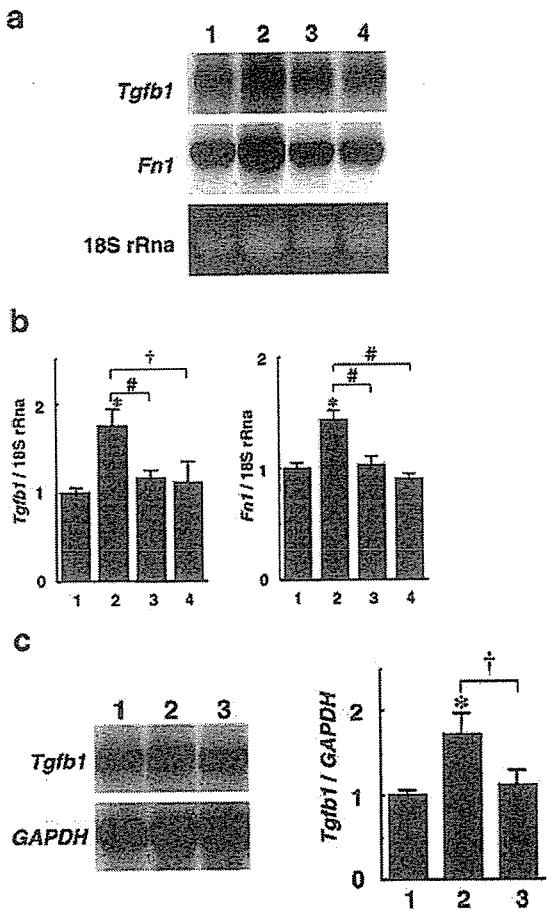

Fig. 7 Representative northern blots for *Tgfb1* and *Fn1* mRNA expression (**a**) and their quantitative analysis (**b**) in cultured mesangial cells under high glucose conditions. 1, normal glucose (5.6 mmol/l); 2, high glucose (25 mmol/l); 3, high glucose+BNP 100 nmol/l; 4, high glucose+cGMP 1 mmol/l. Values are expressed as means±SEM for n=6 in each group. *p<0.01 vs normal glucose; †p<0.02; #p<0.01. **c**. Representative northern blots for *Tgfb1* mRNA expression and quantitative analysis in cultured mesangial cells. 1, normal glucose (5.6 mmol/l); 2, high glucose (25 mmol/l); 3, normal glucose+ mannitol (19.4 mmol/l). Values are expressed as means±SEM for n=4 for each group. *p<0.02 vs normal glucose. †p<0.05

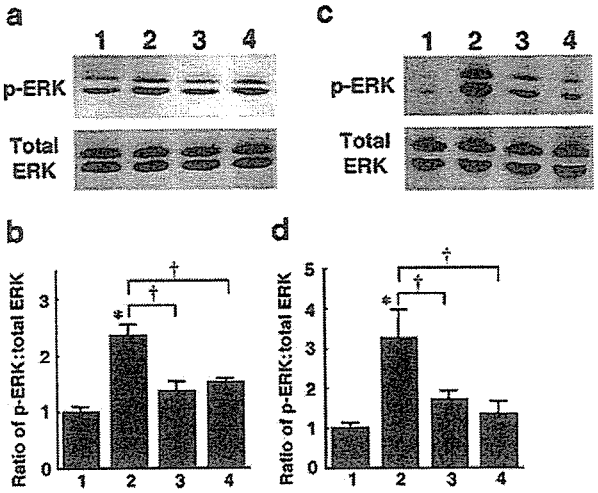

Fig. 8 **a**, **b** Inhibitory effects of BNP on ERK phosphorylation in cultured mesangial cells under high glucose conditions. 1, normal glucose (5.6 mmol/l); 2, high glucose (25 mmol/l); 3, high glucose+ BNP 100 nmol/l; 4, high glucose+cGMP 1 mmol/l. Values are expressed as means±SEM for n=4 in each group. *p<0.01 vs normal glucose; †p<0.01. **c**, **d**. Inhibitory effects of BNP on PMA-induced ERK phosphorylation. 1, control; 2, PMA 100 nmol/l; 3, PMA 100 nmol/l+BNP 100 nmol/l; 4, PMA 100 nmol/l+cGMP 0.1 mmol/l. Values are expressed as means±SEM for n=4 in each group. *p<0.01 vs control; †p<0.01

We also demonstrated that BNP effectively inhibited ERK phosphorylation, as well as TGF-β expression, in cultured mesangial cells under high glucose conditions (Figs 7, 8). High glucose conditions activate PKC, and ERK activation occurs through a PKC-dependent mechanism [31, 37]. BNP also attenuated PKC-induced phosphorylation of ERK. It has been reported that ANP inhibits MAPK activation downstream of PKC via MAPK phosphatase activation in a cGMP-dependent manner [37]. These results therefore suggest that BNP exerts renoprotective effects in diabetes at least partly by locally inhibiting activation of the PKC-ERK pathway at the mesangium. The pathogenic role of PKC in matrix gene activation, haemodynamic abnormalities and proteinuria in vivo has already been shown in diabetic rodent models using a PKC β inhibitor [38, 39].

Podocytes are highlighted as the key in maintaining normal glomerular function and structure [40, 41], and podocyte loss or injury is closely associated with diabetic glomerular injury [42]. Natriuretic peptides act on podocytes and may modulate their function [43], but how natriuretic peptides affect podocytes in diabetic states or whether BNP exerted beneficial effects against podocyte injury in the current study are unclear. Further studies are needed to explore the effects of BNP on podocytes during the course of diabetic nephropathy.

The effect of BNP on glycaemic control is another issue to be addressed. Natriuretic peptides generally act to antagonise the systemic and local actions of angiotensin II [9]; they are therefore considered as endogenous RAS inhibitors. Growing evidence suggests that inhibition of the RAS exerts a beneficial effect on glycaemic control in experimental models and in clinical studies [44–46]. In the present study, we found no significant difference in blood glucose levels between non-Tg and BNP-Tg mice in this type of insulin-deficient model (Table 1). Whether natriuretic peptides or agonists of this system are beneficial in terms of regulating glycaemic control and preventing diabetic complications requires further investigation.

We have previously reported that BNP-Tg mice with higher copy numbers of the transgene show marked skeletal overgrowth [47], indicating that BNP likely activates the

physiological CNP/GC-B pathway in the bone to stimulate endochondral ossification [48]. Therefore, it is important to clarify whether the beneficial effects of BNP observed in this study are GC-A-dependent or GC-B-dependent. In the kidney, GC-A is localised in the mesangium, capillary and tubules, whereas GC-B is localised in the tubular system [11]. In the present study, BNP inhibited glomerular ERK activation and *Tgfb1* expression, suggesting that the effects of BNP were mediated via GC-A. However, it should be noted that the cultured mesangial cells used in our study express both GC-A and GC-B, where CNP has potent antifibrotic effects [24]; therefore the observed in vitro effects of BNP might also be exerted via GC-B. Analyses of crosses between BNP-Tg mice and GC-A null mice [10] and other combinations would answer these questions.

In summary, we demonstrate that a chronic excess of BNP in mice prevents diabetic glomerular injury, with amelioration of albuminuria and renal dysfunction, and these effects may be beyond those from mere systemic blood pressure reduction. Although we need to be cautious in interpreting these results and extrapolating them to clinical situations, our study opens up the possibility that the renoprotective effects of natriuretic peptides may be therapeutically applicable for the prevention of progression of diabetic nephropathy.

Acknowledgements We gratefully acknowledge J. Nakamura and A. Wada for technical assistance, and S. Doi and A. Sonoda for secretarial assistance. This work was supported in part by research grants from the Japanese Ministry of Education, Culture, Sports, Science and Technology, the Japanese Ministry of Health, Labour and Welfare, 'Research for the Future (RFTF)' Programme of the Japan Society for the Promotion of Science, Smoking Research Foundation, and the Salt Science Research Foundation.

References

1. Remuzzi G, Schieppati A, Ruggenenti P (2002) Nephropathy in patients with type 2 diabetes. N Engl J Med 346:1145–1151
2. Parving HH, Mauer M, Ritz E (2004) Diabetic nephropathy. In: Brenner BM (ed). The Kidney. 7th Edition. WB Saunders, Philadelphia, pp 1777–1818
3. Ziyadeh FN, Sharma K (2003) Overview: combating diabetic nephropathy. J Am Soc Nephrol 14:1355–1357
4. The Diabetes Control and Complications Trial Research Group (1993) The effect of intensive treatment of diabetes on the development and progression of long-term complications in insulin-dependent diabetes mellitus. N Engl J Med 329:977–986
5. Fioretto P, Steffes MW, Sutherland DER, Goetz FC, Mauer SM (1998) Reversal of lesions of diabetic nephropathy after pancreas transplantation. N Engl J Med 339:69–75
6. UK Prospective Diabetes Study Group (1998) Tight blood pressure control and risk of macrovascular and microvascular complications in type 2 diabetes: UKPDS 38. BMJ 317:703–713
7. Brenner BM, Cooper ME, de Zeeuw D et al (2001) Effects of losartan on renal and cardiovascular outcomes in patients with type 2 diabetes and nephropathy. N Engl J Med 345:861–869
8. Brownlee M (2001) Biochemistry and molecular cell biology of diabetic complications. Nature 414:813–820
9. Nakao K, Ogawa Y, Suga S, Imura H (1992) Molecular biology and biochemistry of the natriuretic peptide system. I: Natriuretic peptides. J Hypertens 10:907–912
10. Lopez MJ, Wong SK, Kishimoto I et al (1995) Salt-resistant hypertension in mice lacking the guanylyl cyclase-A receptor for atrial natriuretic peptide. Nature 378:65–68
11. Nakao K, Itoh H, Saito Y, Mukoyama M, Ogawa Y (1996) The natriuretic peptide family. Curr Opin Nephrol Hypertens 5:4–11
12. Mukoyama M, Nakao K, Hosoda K et al (1991) Brain natriuretic peptide as a novel cardiac hormone in humans: evidence for an exquisite dual natriuretic peptide system, atrial natriuretic peptide and brain natriuretic peptide. J Clin Invest 87:1402–1412
13. Drewett JG, Garbers DL (1994) The family of guanylyl cyclase receptors and their ligands. Endocr Rev 15:135–162
14. Trevisan R, Fioretto P, Semplicini A et al (1990) Role of insulin and atrial natriuretic peptide in sodium retention in insulin-treated IDDM patients during isotonic volume expansion. Diabetes 39:289–298
15. Yano Y, Katsuki A, Gabazza EC et al (1999) Plasma brain natriuretic peptide levels in normotensive noninsulin-dependent diabetic patients with microalbuminuria. J Clin Endocrinol Metab 84:2353–2356
16. Zietse R, Weimar W, Schalekamp MA (1997) Atrial natriuretic peptide in diabetic nephropathy. Kidney Int 60:S33–S41
17. Tarnow L, Hildebrandt P, Hansen BV, Borch-Johnsen K, Parving HH (2005) Plasma N-terminal pro-brain natriuretic peptide as an independent predictor of mortality in diabetic nephropathy. Diabetologia 48:149–155
18. Ortola FV, Ballermann BJ, Anderson S, Mendez RE, Brenner BM (1987) Elevated plasma atrial natriuretic peptide levels in diabetic rats: potential mediator of hyperfiltration. J Clin Invest 80:670–674
19. Zhang PL, Mackenzie HS, Troy JL, Brenner BM (1994) Effects of an atrial natriuretic peptide receptor antagonist on glomerular hyperfiltration in diabetic rats. J Am Soc Nephrol 4:1564–1570
20. Nakamoto M, Shapiro JI, Shanley PF, Chan L, Schrier RW (1987) In vitro and in vivo protective effect of atriopeptin III on ischemic acute renal failure. J Clin Invest 80:698–705
21. Allgren RL, Marbury TC, Rahman SN et al (1997) Anaritide in acute tubular necrosis. N Engl J Med 336:828–834
22. Ogawa Y, Itoh H, Tamura N et al (1994) Molecular cloning of the complementary DNA and gene that encode mouse brain natriuretic peptide and generation of transgenic mice that overexpress the brain natriuretic peptide gene. J Clin Invest 93:1911–1921
23. Kasahara M, Mukoyama M, Sugawara A et al (2000) Ameliorated glomerular injury in mice overexpressing brain natriuretic peptide with renal ablation. J Am Soc Nephrol 11:1691–1701
24. Suganami T, Mukoyama M, Sugawara A et al (2001) Overexpression of brain natriuretic peptide in mice ameliorates immune-mediated renal injury. J Am Soc Nephrol 12:2652–2663
25. Makino H, Tanaka I, Mukoyama M et al (2002) Prevention of diabetic nephropathy in rats by prostaglandin E receptor EP_1-selective antagonist. J Am Soc Nephrol 13:1757–1765
26. Ishibashi R, Tanaka I, Kotani M et al (1999) Roles of prostaglandin E receptors in mesangial cells under high-glucose conditions. Kidney Int 56:589–600
27. Yamamoto T, Nakamura T, Noble NA, Ruoslahti E, Border WA (1993) Expression of transforming growth factor β is elevated in human and experimental diabetic nephropathy. Proc Natl Acad Sci USA 90:1814–1818
28. Ziyadeh FN, Hoffman BB, Han DC et al (2000) Long-term prevention of renal insufficiency, excess matrix gene expression, and glomerular mesangial matrix expansion by treatment with monoclonal antitransforming growth factor-β antibody in *db/db* diabetic mice. Proc Natl Acad Sci USA 97:8015–8020

29. Tomlinson DR (1999) Mitogen-activated protein kinase as glucose transducers for diabetic complications. Diabetologia 42: 1271–1281
30. Isono M, De La Cruz MC, Chen S, Hong SW, Ziyadeh FN (2000) Extracellular signal-regulated kinase mediates stimulation of TGF-β1 and matrix by high glucose in mesangial cells. J Am Soc Nephrol 11:2222–2230
31. Toyoda M, Suzuki D, Honma M et al (2004) High expression of PKC-MAPK pathway mRNAs correlates with glomerular lesions in human diabetic nephropathy. Kidney Int 66:1107–1114
32. Fujihara CK, Padiha RM, Zats R (1992) Glomerular abnormalities in long-term experimental diabetes: role of hemodynamic and nonhemodynamic factors and effects of antihypertensive therapy. Diabetes 41:286–293
33. Pedersen MM, Christiansen JS, Pedersen EB, Mogensen CE (1992) Determinants of intra-individual variation in kidney function in normoalbuminuric insulin-dependent diabetic patients: importance of atrial natriuretic peptide and glycaemic control. Clin Sci 83:445–451
34. Jacobs EMG, Vervoort G, Branten AJW, Klasen I, Smits P, Wetzels JFM (1999) Atrial natriuretic peptide increases albuminuria in type 1 diabetic patients: evidence for blockade of tubular protein reabsorption. Eur J Clin Invest 29:109–115
35. Huang C, Kim Y, Caramori ML et al (2002) Cellular basis of diabetic nephropathy: II. The transforming growth factor-β system and diabetic nephropathy lesions in type 1 diabetes. Diabetes 51:3577–3581
36. Taal MW, Nenov VD, Wong W et al (2001) Vasopeptidase inhibition affords greater renoprotection than angiotensin-converting enzyme inhibition alone. J Am Soc Nephrol 12:2051–2059
37. Sugimoto T, Haneda M, Togawa M et al (1996) Atrial natriuretic peptide induces the expression of MKP-1, a mitogen-activated protein kinase phosphatase, in glomerular mesangial cells. J Biol Chem 271:544–547
38. Koya D, Haneda M, Nakagawa H et al (2000) Amelioration of accelerated diabetic mesangial expansion by treatment with a PKC β inhibitor in diabetic db/db mice, a rodent model for type 2 diabetes. FASEB J 14:439–447
39. Ishii H, Jirousek MR, Koya D et al (1996) Amelioration of vascular dysfunctions in diabetic rats by an oral PKC β inhibitor. Science 272:728–731
40. Kriz W, LeHir M (2005) Pathways to nephron loss starting from glomerular diseases: insights from animal models. Kidney Int 67:404–419
41. Koshikawa M, Mukoyama M, Mori K et al (2005) Role of p38 mitogen-activated protein kinase activation in podocyte injury and proteinuria in experimental nephrotic syndrome. J Am Soc Nephrol 16:2690–2701
42. Pagtalunan ME, Miller PL, Jumping-Eagle S et al (1997) Podocyte loss and progressive glomerular injury in type II diabetes. J Clin Invest 99:342–348
43. Lewko B, Endlich N, Kriz W, Stepinski J, Endlich K (2004) C-type natriuretic peptide as a podocyte hormone and modulation of its cGMP production by glucose and mechanical stress. Kidney Int 66:1001–1008
44. Higashiura K, Ura N, Takada T et al (2000) The effects of an angiotensin-converting enzyme inhibitor and an angiotensin II receptor antagonist on insulin resistance in fructose-fed rats. Am J Hypertens 13:290–297
45. Shiuchi T, Iwai M, Li HS et al (2004) Angiotensin II type-1 receptor blocker valsartan enhances insulin sensitivity in skeletal muscles of diabetic mice. Hypertension 43:1003–1010
46. Lindholm LH, Ibsen H, Borch-Johnsen K et al (2002) Risk of new-onset diabetes in the Losartan Intervention For Endpoint reduction in hypertension study. J Hypertens 20:1879–1886
47. Suda M, Ogawa Y, Tanaka K et al (1998) Skeletal overgrowth in transgenic mice that overexpress brain natriuretic peptide. Proc Natl Acad Sci USA 95:2337–2342
48. Yasoda A, Komatsu Y, Chusho H et al (2004) Overexpression of CNP in chondrocytes rescues achondroplasia through a MAPK-dependent pathway. Nat Med 10:80–86

Osteoporos Int (2006) 17: 1103–1110
DOI 10.1007/s00198-006-0091-4

ORIGINAL ARTICLE

Negative correlation between bone mineral density and TSH receptor antibodies in male patients with untreated Graves' disease

T. Majima · Y. Komatsu · K. Doi · C. Takagi · M. Shigemoto · A. Fukao · T. Morimoto · J. Corners · K. Nakao

Received: 8 June 2005 / Accepted: 10 February 2006 / Published online: 7 April 2006

Abstract *Introduction:* Although it has been established that hyperthyroidism leads to reduced bone mineral density (BMD), with accelerated bone turnover promoting bone resorption in female patients, there is a dearth of data for male patients with hyperthyroidism. This study evaluated BMD and bone metabolism in male patients with Graves' disease. *Methods:* The study included 56 Japanese male patients with newly diagnosed Graves' disease and 34 normal Japanese male control subjects of similar age and body mass index. We used dual energy x-ray absorptiometry to measure BMD at sites with different cortical/cancellous bone ratios (lumbar spine, femoral neck, and distal radius). *Results:* At the lumbar spine and the distal radius, BMD and T-scores were significantly lower for patients than for controls. At the femoral neck, on the other hand, the same values were relatively, but not significantly, lower in patients than in controls. However, Z-scores at all three sites were significantly lower for patients than for controls. The Z -score at the distal radius of patients was significantly lower than that at their lumbar spine and femoral neck. In addition, Z-score at the distal radius correlated negatively with age, free thyroxine, thyroid stimulating hormone receptor antibodies, thyroid stimulating antibody, and urinary N-terminal telopeptide of type I collagen normalized by creatinine. *Conclusions:* These results indicate a high prevalence of cortical bone loss in male patients with Graves' disease, especially elderly patients. We conclude that BMD measurement is crucial in all Graves' disease patients regardless of their gender and that the radial BMD as well as BMD at the lumbar spine and femoral neck should be monitored to effectively prevent bone loss and subsequent fracture.

Keywords Bone mineral density · Distal radius · Graves' disease · Male patients · TSH receptor antibodies

T. Majima · K. Doi · C. Takagi · M. Shigemoto
Department of Endocrinology and Metabolism,
Rakuwakai Otowa Hospital,
Kyoto, Japan

Y. Komatsu (✉) · K. Nakao
Department of Medicine and Clinical Science,
Kyoto University Graduate School of Medicine,
54 Shogoin Kawahara-cho Sakyo-ku,
Kyoto 606-8507, Japan
e-mail: komatsuy@barium.rirc.kyoto-u.ac.jp
Tel.: +81-75-7513168
Fax: +81-75-7719452

A. Fukao
Department of Psychosomatic Medicine,
Rakuwakai Otowa Hospital,
Kyoto, Japan

T. Morimoto
Department of General Medicine,
Kyoto University Graduate School of Medicine,
Kyoto, Japan

J. Corners
Rakuwakai Otowa Hospital,
Kyoto, Japan

Introduction

Reduction in bone mineral density (BMD) following hyperthyroidism in female subjects has been described in many reports [1–7]. However, as Greenspan et al. [8] mentioned in their review of the published data, far fewer studies have been conducted for male subjects. Although normal BMD has been reported in male patients with subclinical hyperthyroidism [9–11], only limited information is available on BMD in men with active hyperthyroidism. In addition, interpretation of the effects of hyperthyroidism on bone metabolism is hampered by the background of involutional osteoporosis in female patients [12]. In this study, we therefore examined the BMD of male patients, in whom the influence of involutional osteoporosis should be much less, who had newly diagnosed and

untreated Graves' disease (GD) accompanied by active hyperthyroidism.

A bone histomorphometric study of hyperthyroidism has shown that the increase in osteoclastic resorption is more prominent in cortical than in cancellous bone [13], so that bone loss, especially in cortical bone, is considered one of the characteristics of osteoporosis resulting from hyperthyroidism [6, 8]. In patients with hyperthyroidism, therefore, bone and mineral metabolism at different sites can be expected to be affected differently, depending on the cortical/cancellous bone ratio at a given site. Because previous studies have often examined BMD at a single site, however, we used dual energy x-ray absorptiometry (DXA) to measure BMD of patients with GD at three sites with different cortical/cancellous bone ratios: the lumbar spine (LS), the femoral neck (FN), and the distal third of the radius (DR). We also assessed the relationship among BMD values at the three sites and included the clinical parameters—age, thyroid hormone levels, thyroid stimulating hormone (TSH) receptor antibodies (TRAb), thyroid stimulating antibody (TSAb), and bone markers—that have often been reported as risk factors for reduced BMD in hyperthyroidism [4, 5, 14–20].

The purpose of our study was to determine 1) whether BMD decreases and bone turnover increases in male patients with overt hyperthyroidism associated with GD, as has been determined in female patients, 2) whether BMD at different sites is affected differently by hyperthyroidism, 3) which patients with overt hyperthyroidism associated with GD are more likely to have reduced BMD, and 4) whether TRAb or TSAb, or both, influence bone metabolism and BMD in untreated GD.

Subjects and methods

Subjects

The study included 56 Japanese men (mean age 43.6±10.0 years) with newly diagnosed GD who were treated at the Clinic of Rakuwakai Otowa Hospital between April 2003 and January 2005. Their clinical data are shown in Table 1. The diagnosis of GD was established on the basis of clinical signs and symptoms and laboratory test results, including positivity for TSAb and/or TRAb and an elevated technetium-99m thyroid scan (>5%). The control group comprised 34 Japanese healthy male volunteers without past or present history of thyroid disease; they were all employees of Rakuwakai Otowa Hospital and were similar to the patients in age, height, and weight (Table 1). Study and control group subjects were also similar in exercise history and calcium intake.

All subjects completed a questionnaire administered by the physician or nurse and underwent laboratory blood tests. We excluded subjects who had a history of fracture or disease (liver disease, renal dysfunction, malignancy, diabetes mellitus, hyperparathyroidism, hypercorticoidism, or hypogonadism) and those taking medications that could influence bone metabolism (active vitamin D3, bisphosphonates, calcitonin, testosterones, steroids, thyroid hormones, diuretics, heparin, or anticonvulsants). All subjects underwent plain x-ray (anteroposterior and lateral views) of the LS, and those found to have scoliosis, compression fractures, or ectopic calcifications that could interfere with the bone mineral results were excluded. None of the subjects were smokers or alcoholics.

This study was approved by the ethics committee of Rakuwakai Otowa Hospital, and all participants provided written informed consent.

Table 1 Characteristics of the subjects (*BMI* body mass index, *FT3* free T3, *FT4* free T4, *TRAb* TSH receptor antibodies, *TSAb* thyroid stimulating antibody, *ALP* alkaline phosphatase, *BAP* bone-specific alkaline phosphatase, *U.NTx* N-terminal telopeptide of type I collagen normalized by creatinine, ND not done)

	Graves' disease (n=56)	Control (n=34)	P-value
Age (years)	43.6±10.0[a]	43.8±10.5	0.9437
Height (cm)	169.3±5.1[a]	170.1±6.3	0.5051
Weight (kg)	65.8±7.8[a]	66.1±5.2	0.8433
BMI (kg/m^2)	22.9±2.1[a]	22.9±2.0	0.9585
FT3 (pg/ml)	11.71±4.0[b]	3.30±0.48	<0.0001
FT4 (ng/dl)	4.36±1.4[b]	1.34±0.22	<0.0001
TSH (μIU/ml)	<0.01	2.17±0.51	–
TRAb (%)	52.8±20.8	ND	–
TSAb (%)	516.9±206.0	ND	–
Calcium (mg/dl)	9.95±0.31[c]	9.77±0.31	0.0121
AlP (IU/l)	353.6±46.4[b]	199.1±37.0	<0.0001
BAP (U/l)	53.0±9.4[b]	23.8±3.6	<0.0001
U.NTx (nmolBCE/mmolCre)	147.3±26.0[b]	34.6±11.2	<0.0001

Data represents mean±SD
P-values for comparisons between patients with Graves' disease and controls: [a]NS, $P>0.05$, [b]$P<0.01$, [c]$P<0.05$

BMD measurements

BMD was measured at the LS (L2-L4), the FN, and DR by DXA (Hologic QDR 4,500c; Hologic, Waltham, MA, USA). To avoid technical discrepancies, the same operator measured all the subjects. Values of BMD at the LS were calculated as the mean of those at L2-L4, and T-scores and Z-scores were calculated on the basis of the normal reference values of the age- and gender-matched Japanese group provided by the DXA system manufacturer.

Biochemical measurements

Serum samples were obtained before 0800 after overnight fasting and were immediately processed and kept frozen at −20°C until the assays were done. Serum free T3 (FT3), free T4 (FT4), and TSH were measured with the aid of an electrochemiluminescence immunoassay (ECLUSISU; Roche Diagnostics, Tokyo, Japan; normal values: FT3,

2.30–4.30 pg/ml; FT4, 0.90–1.70 ng/dl; TSH 0.500–5.000 μIU/ml). The minimum detection limit of the TSH assay was 0.005 μIU/ml. TRAb was measured with a radioreceptor assay (COSMIC III; Cosmic, Tokyo, Japan; normal range 0.0–15.0%), and TSAb with a bioassay radioimmunoassay (TSAB-Kit-Yamasa; Yamasa, Chiba, Japan; normal range <180%). Serum calcium, phosphate, creatinine, and alkaline phosphatase (ALP) were measured by using standard laboratory methods. Bone-specific alkaline phosphatase (BAP) was measured with an enzyme immunoassay kit (Osteolinks-BAP; Sumitomo Pharmaceuticals, Tokyo, Japan; normal range 13.0–33.9 U/l) as a marker of bone formation. Urinary N-terminal telopeptide of type I collagen normalized by creatinine (U.NTx) was measured in the morning in the second voided urine sample by means of an enzyme-linked immunosorbent assay (OSTEOMARK; Mochida Pharmaceutical, Tokyo, Japan; normal range 13.0–66.2 nmolBCE/mmolCre) as a marker of bone resorption.

Statistical analysis

Data were analyzed by *t*-test for differences between two groups, by one-way factorial ANOVA and Fisher's protected least significant difference (PLSD) method for differences among three groups, and by Pearson's correlation test for determining correlations. Statistics were calculated with Statview version 4.0 (Abacus Concepts, Berkeley, CA, USA). A *P*-value <0.05 was considered statistically significant.

Results

Table 1 shows a comparison of GD patients and controls. There were no significant differences between the two groups in age, height, weight, or body mass index (BMI). However, serum calcium, ALP, BAP, and U.NTx levels of the GD patients were significantly higher than those of controls. U.NTx was about four times higher, and BAP was about twice as high. The levels of thyroid hormones were also elevated, while TSH levels were suppressed below sensitivity in all the patients with GD.

Table 2 and Fig. 1 show a comparison of BMD and T- and Z-scores for the patient and control groups. At the LS and the DR, BMD and T-scores were significantly lower for patients than for controls. At the FN, on the other hand, the same values were relatively, but not significantly, lower in patients than in controls. However, Z-scores at all three sites were significantly lower for patients than for controls.

Figure 2a,b shows comparisons of T- and Z-scores among different sites in patients with GD, analyzed by one-way factorial ANOVA and Fisher's PLSD test. Both T-score and Z-score at the DR were significantly lower than those at the LS and FN (P=0.0126 and 0.0008 for T-score, and P<0.0001 and P<0.0001 for Z-score, respectively),

Table 2 Bone mineral density (BMD), T-score, and Z-score at the lumbar spine, the femoral neck, and the distal radius in patients with Graves' disease and control subjects

	Graves' disease	Control	p-value
Lumbar spine			
BMD (g/cm^2)	0.964±0.095[a]	1.016±0.078	0.0085
T-score (SD)	−0.511±0.948[a]	−0.035±0.715	0.0085
Z-score (SD)	−0.280±0.608[a]	0.097±0.501	0.0029
Femoral neck			
BMD (g/cm^2)	0.812±0.089[b]	0.841±0.070	0.1089
T-score (SD)	−0.398±0.701[b]	−0.170±0.549	0.1089
Z-score (SD)	−0.067±0.649[c]	0.192±0.492	0.0486
Distal radius			
BMD (g/cm^2)	0.679±0.074[a]	0.751±0.052	<0.0001
T-score (SD)	−1.015±1.171[a]	0.129±0.823	<0.0001
Z-score (SD)	−0.953±1.009[a]	0.045±0.724	<0.0001

Values are means ± SD
P-values for comparisons between patients with Graves' disease and controls: [a]P<0.01, [b]NS, P>0.05, [c]P<0.05

whereas neither T-score nor Z-score showed any marked differences between the LS and the FN.

Table 3 shows correlations of BMD, T-score, and Z-score with age, height, weight, BMI, and the biochemical parameters in patients with GD. There was a significant negative correlation between age and both BMD and T-score at all three sites. Otherwise, however, there was no statistically significant correlation at either the LS or the FN. On the other hand, Z-scores as well as BMD and T-scores at the DR correlated negatively with FT4, TRAb, TSAb, and U.NTx, but not so at the LS or the FN. These significant negative correlations of the Z-score at the DR with age, FT4, TRAb, TSAb, and U.NTx are shown in Fig. 3.

Furthermore, multiple regression analysis was performed with the Z-score at the DR as the dependent variable and all the clinical parameters listed in Table 3 as the independent variables. A forward stepwise procedure

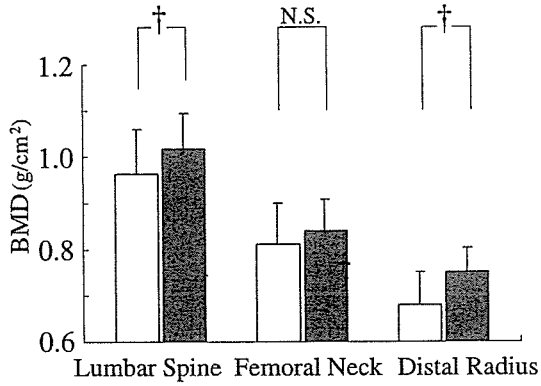

Fig. 1 Comparison of bone mineral density at the lumbar spine, femoral neck and distal radius of patients with Graves' disease (*white columns*) and control subjects (*black columns*). Each column represents the mean ± SD. *P<0.05, †P<0.01

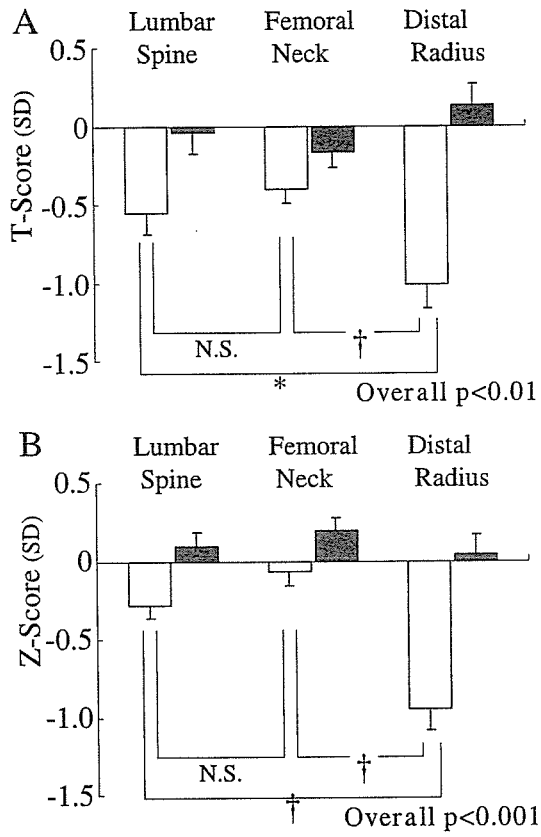

Fig. 2 **a** Comparison of T-scores at the lumbar spine, femoral neck, and distal radius of patients with Graves' disease (*white columns*). **b** Comparison of Z-scores at the lumbar spine, femoral neck, and distal radius of patients with Graves' disease (*white columns*). *Black columns* show data of controls. Each column represents the mean value ± SEM. *$P<0.05$, †$P<0.01$

identified two variables, age and FT4, as significant predictors in the following equation:

$$(R^2 = 0.230, P = 0.0010)$$
$$: predicted\ Z\ score\ at\ the\ DR = 1.657 - 0.227 \times FT4 - 0.032 \times Age.$$

Table 4 shows correlations of bone metabolic markers with thyroid function and thyroid autoantibodies. There was a significant positive correlation between TSAb and U. NTx (Fig. 3). Otherwise, relatively positive correlations between bone metabolic markers with thyroid function and thyroid autoantibodies were found, but none of them reached significance.

Discussion

Most [1–7, 14–16, 21], but not all [20, 22], studies have reported a decrease in BMD in female patients with active hyperthyroidism, as Greenspan et al. [8] reviewed in a metaanalysis of the published data. However, fewer studies have been conducted for men. Only small numbers (from two to eight) of male patients with hyperthyroidism have been examined in some previous studies [14, 15, 20, 21]. In other studies, separate data for the male patients or the actual values of their BMD were unfortunately not given [16, 23]. Indeed, BMD of male subjects on TSH suppressive and replacement levothyroxine therapy or with subclinical hyperthyroidism has been examined in some papers [9–11]. However, there is still little information available in the literature about the BMD of male patients with active hyperthyroidism.

Table 3 Correlations of bone mineral density (BMD) with age, height, weight, body mass index (BMI), and the biochemical parameters in patients with Graves' disease (*FT3* free T3, *FT4* free T4, *TRAb* TSH hormone receptor antibodies, *TSAb* thyroid stimulating antibody, *ALP* alkaline phosphatase, *BAP* bone-specific alkaline phosphatase, *U.NTx* N-terminal telopeptide of type I collagen normalized by creatinine)

	Lumbar spine			Femoral neck			Distal radius		
	BMD	T-score	Z-score	BMD	T-score	Z-score	BMD	T-score	Z-score
Age	−0.443[a]	−0.443[a]	−0.074	−0.471[a]	−0.471[a]	−0.087	−0.461[a]	−0.461[a]	−0.293[b]
Height	0.006	0.006	−0.016	0.052	0.052	0.046	−0.107	−0.107	−0.110
Weight	0.165	0.165	0.118	0.223	0.223	0.203	0.102	0.102	0.111
BMI	0.191	0.191	0.153	0.236	0.236	0.223	0.179	0.179	0.197
FT3	−0.059	−0.059	−0.099	−0.176	−0.176	−0.247	−0.155	−0.155	−0.182
FT4	−0.162	−0.162	−0.204	−0.155	−0.155	−0.211	−0.325[b]	−0.325[b]	−0.359[a]
TRAb	−0.038	−0.038	−0.057	−0.138	−0.138	−0.183	−0.275[b]	−0.275[b]	−0.312[b]
TSAb	−0.102	−0.102	−0.09	−0.115	−0.115	−0.023	−0.315[b]	−0.315[b]	−0.355[a]
Calcium	−0.077	−0.077	−0.117	0.061	0.061	−0.071	0.038	0.038	0.041
ALP	−0.090	−0.090	−0.145	−0.091	−0.091	−0.191	−0.062	−0.062	−0.122
BAP	−0.106	−0.106	−0.103	−0.139	−0.139	−0.145	−0.193	−0.193	−0.200
U.NTx	−0.155	−0.155	−0.135	−0.262	−0.262	−0.260	−0.335[b]	−0.335[b]	−0.324[b]

Values are correlation coefficients
P-values for correlations of BMD with age, height, weight, BMI, and the biochemical parameters in patients with Graves' disease: [a]$P<0.01$, [b]$P<0.05$